Chemistry Research Journal, 2024, 9(1):94-126
Available online www.chemrj.org

Research Article

ISSN: 2455-8990
CODEN(USA): CRJHA5

Quantum-chemical analysis of the relationship between electronic structure and 5-HT_{2A}, 5-HT_{2B} and 5-HT_{2C} receptor binding affinity of a group of *N*-benzyl tryptamines with possible psychedelic and/or hallucinogenic activity

J.S. Gómez-Jeria* and Ignacio Jaramillo-Hormazábal

Quantum Pharmacology Unit, Laboratory of Theoretical Chemistry, Department of Chemistry, Faculty of Sciences, University of Chile. Las Palmeras 3425, Santiago CP 7800003, Chile.
E-mail: facien03@chile.cl (J.S.G.-J.)

Abstract
We present the results of the application of the Klopman-Peradejordi-Gómez QSAR method to the search of relationships between electronic structure and 5-HT_{2A}, 5-HT_{2B} and 5-HT_{2C} receptor binding affinity of a group of N-benzyl tryptamines. Statistically significant results were obtained for the three receptors. An analysis of the results was conducted on the basis of the local molecular orbital structure and the local atomic reactivity indices of the atoms appearing in the resulting QSAR equations. Suggestions about the possible nature of each atom-site interaction were presented. The two-dimensional partial pharmacophores built from the QSAR equation should be of help to synthesize molecules with higher receptor affinity.

Keywords: QSAR, *N*-benzyl tryptamines, 5-HT_{2A} receptor, 5-HT_{2B} receptor, 5-HT_{2C} receptor, serotonin, psychedelics, hallucinogens, KPG method, receptor affinity, Klopman-Peradejordi-Gómez method, electronic structure.

1. Introduction

Serotonin receptors (or 5-HT receptors), belong to the G protein-coupled receptors superfamily. They mediate the effects of serotonin, a neurotransmitter implicated in several physiological phenomena, including appetite, blood pressure, mood, pain, sleep cycle and the regulation of body temperature [1]. As molecules acting at serotonin receptors have been the object of many studies in our Unit we refer the reader to these articles for more information[2-19].

Halberstadt inform us that "one class of hallucinogens are 2,5-dimethoxy-substituted phenethylamines, such as the so-called 2C-X compounds 2,5-dimethoxy-4-bromophenethylamine and 2,5-dimethoxy-4-iodophenethylamine. Addition of an N-benzyl group to phenethylamine hallucinogens produces a marked increase in 5-HT_{2A}-binding affinity and hallucinogenic potency. N-benzylphenethylamines ("NBOMes") such as N-(2-methoxybenzyl)-2,5-dimethoxy-4-iodophenethylamine show subnanomolar affinity for the 5-HT_{2A} receptor and are reportedly highly potent in humans" [20, 21]. It was only a question of time to synthesize different *N*-benzyl tryptamines. For example,

Toro-Sazo et al. synthesized a large number of N-benzyltryptamines and reported their receptor affinity for several serotonin receptors.

This paper reports the results of the application of the Klopman-Peradejordi-Gómez QSAR method to these molecules. We expected to obtain formal equations relating the variation of the affinity for 5-HT_{2A}, 5-HT_{2B} and 5-HT_{2C} receptors with the variation of the numerical values of a large group of local atomic reactivity indices inside each equation.

Molecules and receptor binding affinities.

The molecules and their pK values were obtained from a paper from Toro-Sazo et al.[22] The general formula is shown in Figure 1 and the pK data in Table 1.

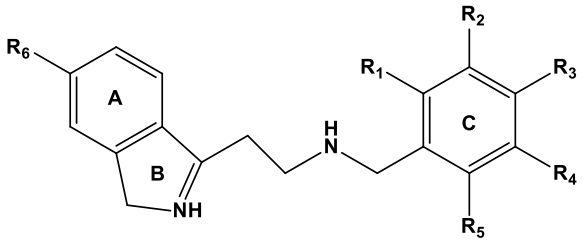

Figure 1: N-benzyltryptamines

Table 1: N-benzyltryptamines and receptor binding affinities

Molecule	R_1	R_2	R_3	R_4	R_5	R_6	pK 5-HT_{2A}	pK 5-HT_{2B}	pK 5-HT_{2C}
1	H	H	H	H	H	H	6.61	7	6.73
2	OH	H	H	H	H	H	6.94	7.17	7.07
3	OMe	H	H	H	H	H	7.05	7.33	6.65
4	Me	H	H	H	H	H	-------	6.47	6.18
5	Cl	H	H	H	H	H	7.92	7.63	7.61
6	Br	H	H	H	H	H	6.71	7.13	6.47
7	H	OH	H	H	H	H	7.12	7.43	7.59
8	H	Me	H	H	H	H	7.84	7.77	7.13
9	H	F	H	H	H	H	6.59	6.9	6.67
10	H	Cl	H	H	H	H	7.35	7.46	7.01
11	H	Br	H	H	H	H	8.09	7.66	7.12
12	H	H	OH	H	H	H	6.04	6.31	6
13	H	H	OMe	H	H	H	6.34	7.16	6.45
14	H	H	Me	H	H	H	6.38	7.13	6.48
15	H	H	OEt	H	H	H	6.56	6.57	6.13
16	H	H	Cl	H	H	H	6.15	6.65	6.02
17	H	H	Br	H	H	H	6	6.58	5.97
18	H	H	NO_2	H	H	H	5.58	6.7	5.85
19	OH	OMe	H	H	H	H	7.85	7.88	7.78
20	OMe	OMe	H	H	H	H	5.82	6.71	5.95
21	OH	Br	H	H	H	H	7.85	7.81	6.86
22	OH	F	H	H	H	H	6.68	6.89	6.75
23	OH	H	H	Me	H	H	6.13	6.81	6.57
24	OH	H	H	H	H	H	6.12	7.11	6.98
25	OMe	H	H	F	H	H	6.44	7.02	6.82
26	OH	H	H	Br	H	H	6.51	------	6.14
27	OMe	H	H	Br	H	H	5.95	7.04	6.87
28	OMe	H	H	Cl	H	H	6.01	6.1	5.88
29	OMe	H	H	OMe	H	H	6.48	7.24	7.06
30	OH	H	H	NO_2	H	H	-------	6.05	--------
31	OH	H	Br	H	H	H	5.81	6.96	6.22

32	OMe	H	OMe	H	H	H	6.18	6.63	6.57
33	OH	H	H	H	Br	H	5.78	7.16	6.95
34	OH	H	H	H	F	H	6.64	6.94	6.81
35	OH	Br	H	Br	H	H	-------	5.22	--------
36	H	OMe	OMe	H	H	H	5.89	6.54	5.92
37	H	H	H	H	H	OMe	7.48	7.78	7.02
38	OMe	H	H	H	H	OMe	7.35	7.8	7.16
39	Cl	H	H	H	H	OMe	7.87	7.43	7.13
40	Br	H	H	H	H	OMe	7.91	7.54	7.15
41	H	H	Br	H	H	OMe	6.41	6.81	6.42
42	OH	H	H	OMe	H	OMe	6.87	7.69	7.39
43	OH	H	H	F	H	OMe	8.4	8.05	7.4
							n=40	n=42	n=41

The next figures show the histogram of frequencies and the Box-Whiskers plot of values binding data for the three receptors. This is to give a general information about the data. The Box-Whiskers plot makes it easy to spot outliers and extreme values that should not be omitted from the original set of values.

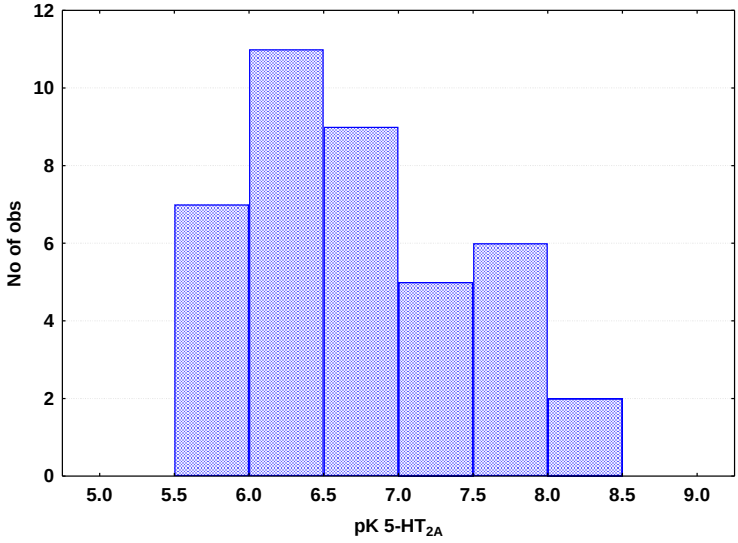

Figure 2:-HT_{2A} receptor data. Histogram of frequencies

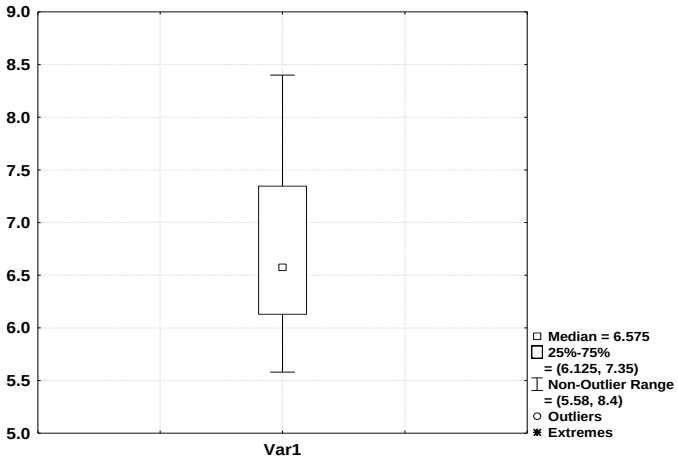

Figure 3: HT_{2A} receptor data. Box-Whiskers plot

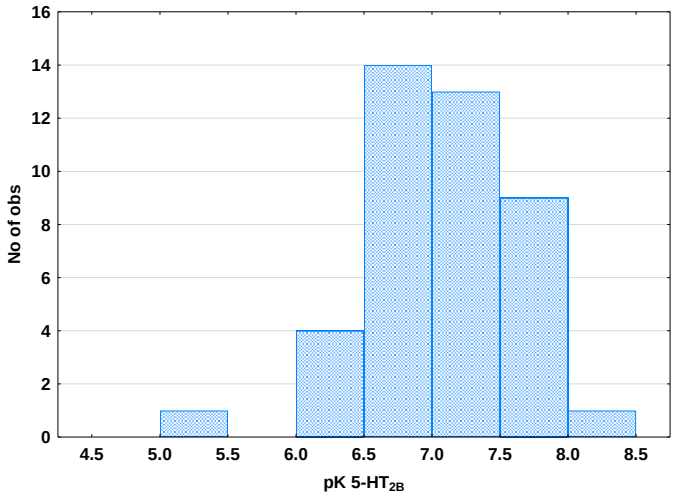

Figure 4: HT_{2B} receptor data. Histogram of frequencies

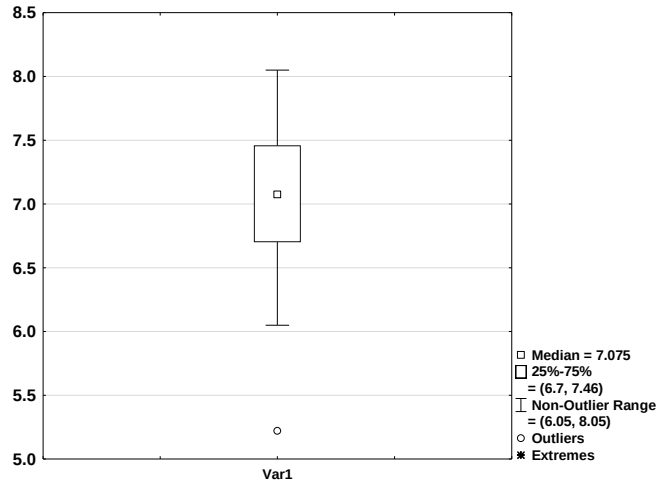

Figure 5: HT_{2B} receptor data. Box-Whiskers plot

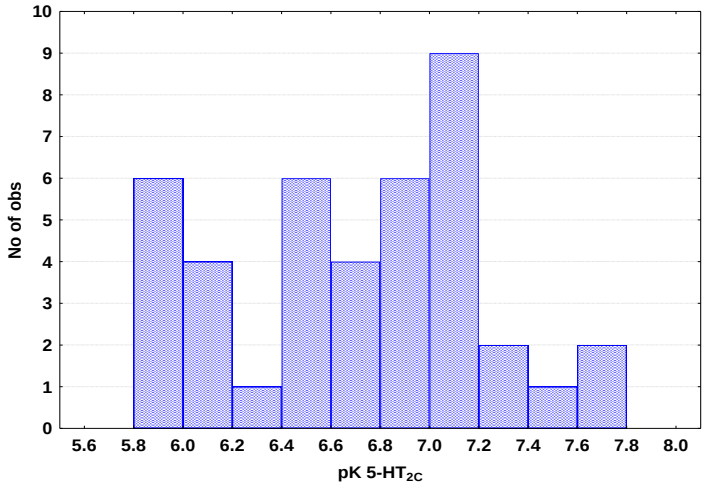

Figure 6: HT_{2C} receptor data. Histogram of frequencies

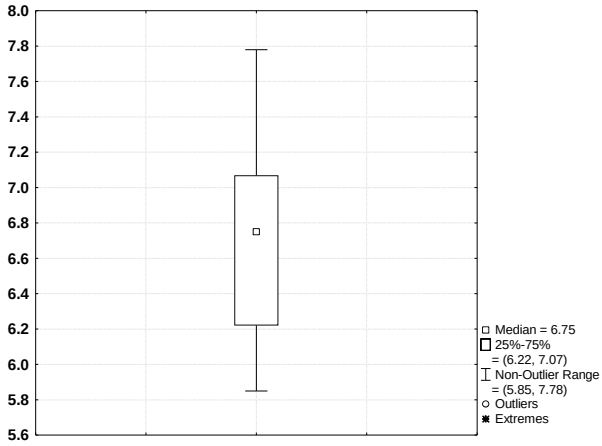

Figure 7: HT_{2C} receptor data. Box-Whiskers plot

Models.

The Klopman-Peradejordi-Gómez (KPG) QSAR method is based on the following linear equation [23-32]:

$$\log(BA)=a+b\log\left(M_D\right)+\sum_{o=1}^{sub}\varphi_o+\sum_{i=1}^{Y}\left[e_iQ_i+f_iS_i^E+s_iS_i^N\right]+$$
$$+\sum_{i=1}^{Y}\sum_{m=(HOMO-2)^*,i}^{(HOMO)^*,i}\left[h_i\left(m\right)F_i(m^*)+j_i\left(m\right)S_i^E\left(m^*\right)\right]+$$
$$+\sum_{i=1}^{Y}\sum_{m'=(LUMO)^*,i}^{(LUMO+2)^*,i}\left[r_i\left(m'\right)F_i(m'^*)+t_i\left(m'\right)S_i^N\left(m'^*\right)\right]+ \quad (1)$$
$$+\sum_{i=1}^{Y}\left[g_i\mu_i^*+k_i\eta_i^*+o_i\omega_i^*+z_i\zeta_i^*+w_jQ_i^{*,max}\right]$$

where BA is a biological activity, M_D is the drug's mass and φ_o is the orientational parameter of the o-th substituent (the summation runs over all the substituents selected for the research). Q_i is the net charge of atom i and S_i^E and S_i^N are, respectively, the total atomic electrophilic and nucleophilic superdelocalizabilities of atom i. F_{i,m^*} is the electron population of atom i in occupied (empty) local MO m* (m'*), $S_i^E(m)^*$ is the orbital electrophilic superdelocalizability at occupied local MO m* of atom i and $S_i^N(m')^*$ is the orbital nucleophilic superdelocalizability at empty local MO m'* of atom i. μ_i^*, η_i^*, ω_i^*, ζ_i^* and $Q_i^{*,max}$ are, respectively, the local atomic electronic chemical potential, the local atomic hardness, the local atomic electrophilicity, the local atomic softness and the maximal amount of electronic charge that atom i may accept. These indices were developed within the Hartree-Fock formalism. The molecular orbitals with an asterisk are the Local Molecular Orbitals (LMO) of each atom. For atom x, the LMOs are defined as the subset of the molecule's MOs having an electron population greater than 0.01e on x. In this study we have considered the three highest occupied *local* MOs ((HOMO)*, (HOMO-1)*, (HOMO-2)*) and the three lowest empty local MOs ((LUMO)*, (LUMO+1)*, (LUMO+2)*) of each atom because experimental evidence indicates that they are determinant for molecular reactivity. The index Y in the summations runs over all atoms composing the molecule. Excellent results were obtained for different molecular systems and biological activities.

Electronic Structure Calculations

The electronic structure of all molecules was calculated within the Density Functional Theory (DFT) at the B3LYP/6-31g(d,p) level after full geometry optimization. The Gaussian suite of programs was used [33]. All the information needed to calculate the values of the local atomic reactivity indices was obtained from the Gaussian results with the D-Cent-QSAR software[34]. All the electron populations smaller than or equal to 0.01 e were considered as zero. Negative electron populations originating from Mulliken Population Analysis were corrected as usual[35]. We employed Linear Multiple Regression Analysis (LMRA) techniques to find the best solution. For each case, a matrix containing the dependent variable (the receptor binding affinity of each case) and the local atomic reactivity indices of all atoms of the common skeleton as independent variables was created. The Statistica software was utilized for LMRA[36].

The reader should notice that to solve the system of equations 1 necessarily we must use the same number of atoms for each molecule (i.e., index Y in Eq. 1 must be the same for all molecules). For this reason, we introduced the concept of *common skeleton*. It corresponds to a definite collection of atoms, common to all molecules analyzed, that supposedly accounts for nearly all the biological activity. The action of the substituents consists in modifying the electronic structure of the common skeleton and influencing the right alignment of the drug throughout the orientational parameters. It is hypothesized that different parts or this common skeleton accounts for almost all the interactions leading to the expression of a given biological activity. The common skeleton for N-benzyltryptamines is shown in Fig. 8.

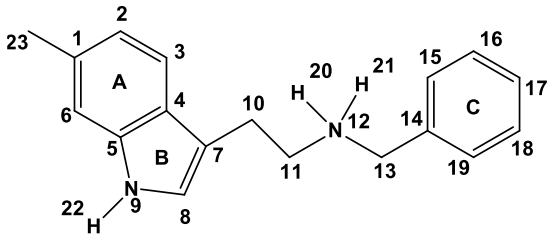

Figure 8: Common skeleton numbering

Results

Results for the 5-HT$_{2A}$ receptor.

The best equation found is:

$$pK_i = 13.41 - 5.25S_9^E(\text{HOMO-1})^* - 0.11S_{20}^N(\text{LUMO+1})^* - 3.28Q_{13}^{*,max} + 0.75\eta_{14} - 1.69F_{16}(\text{HOMO})^* - 26.35Q_{20} + 7.06S_{21}^E(\text{HOMO})^* \quad (2)$$

with n=33, R=0.95, R^2=0.92, adj-R^2=0.89, F(7,24)=39.664 (p<0.000001) and SD=0.20. No outliers were detected, and no residuals fall outside the ±2σ limits. Here, S_9^E(HOMO-1)* is the electrophilic superdelocalizability of the second highest local MO of atom 9, S_{20}^N(LUMO+1)* is the nucleophilic superdelocalizability of the second lowest empty MO localized on atom 20, $Q_{13}^{*,max}$ is the is the maximum amount of electronic charge that atom 13 can accept, η_{14} is the local atomic hardness of atom 14, F_{16}(HOMO)* is the electron population of the highest occupied MO localized on atom 16 (the Fukui index), Q_{20} is the net charge of atom 20 and S_{21}^E(HOMO)* is the electrophilic superdelocalizability of the highest occupied MO localized on atom 21.

Tables 2 and 3 show the beta coefficients, the results of the t-test for significance of coefficients and the matrix of squared correlation coefficients for the variables of Eq. 2. Figure 9 displays the plot of observed *vs.* calculated binding affinities.

Table 2: Beta coefficients and t-test for significance of coefficients in Eq. 2.

Variable	Beta	t(25)	p-level
S_9^E(HOMO-1)*	-0.51	-6.87	0.000000
S_{20}^N(LUMO+1)*	-0.47	-6.85	0.000000
$Q_{13}^{*,max}$	-0.45	-7.04	0.000000
η_{14}	0.40	5.91	0.000004
F_{16}(HOMO)*	-0.41	-5.05	0.000033
Q_{20}	-0.29	-3.65	0.001
S_{21}^E(HOMO)*	0.22	2.83	0.009

Table 3: Matrix of squared correlation coefficients for the variables in Eq. 2.

	S_9^E(HOMO-1)*	**S_{20}^N(LUMO+1)***	**$Q_{13}^{*,max}$**	**η_{14}**	**F_{16}(HOMO)***	**Q_{20}**
S_{20}^N(LUMO+1)*	0.03	1				
$Q_{13}^{*,max}$	0.05	0.09	1			
η_{14}	0.08	0.02	0.00	1		
F_{16}(HOMO)*	0.02	0.03	0.04	0.06	1	
Q_{20}	0.16	0.00	0.01	0.01	0.32	1
S_{21}^E(HOMO)*	0.21	0.18	0.01	0.16	0.02	0.01

A 0.00 with any number of decimal places found in any Table and similar ones means that the actual value is lesser than the table value.

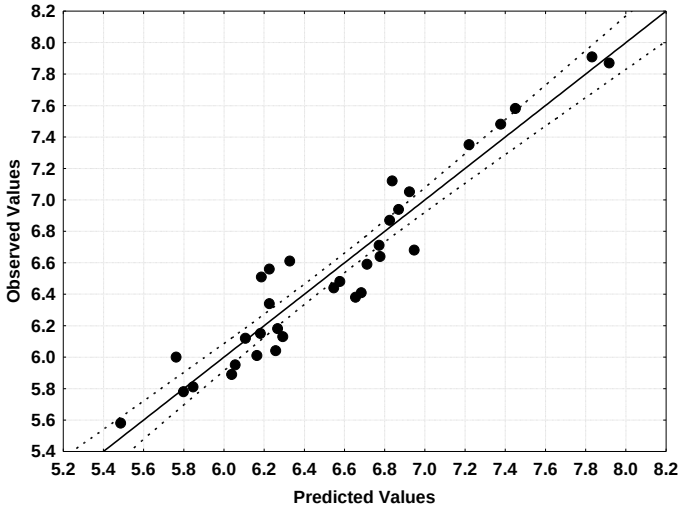

Figure 9: Plot of predicted vs. observed pK_i values (Eq. 2). Dashed lines denote the 95% confidence interval.

The associated statistical parameters of Eq. 2 indicate that this equation is statistically significant and that the variation of the numerical values of a group of seven local atomic reactivity indices of atoms constituting the common skeleton explains about 89% of the variation of pK values. Figure 9, spanning about 2.1 orders of magnitude, shows that there is a good correlation of observed *versus* calculated values. Table 3 shows no significant correlations among independent variables.

The next two figures show the histogram of frequencies and the Box-Whiskers plot of values with median and quartile values for the data set (n=33) used to obtain Eq. 2.

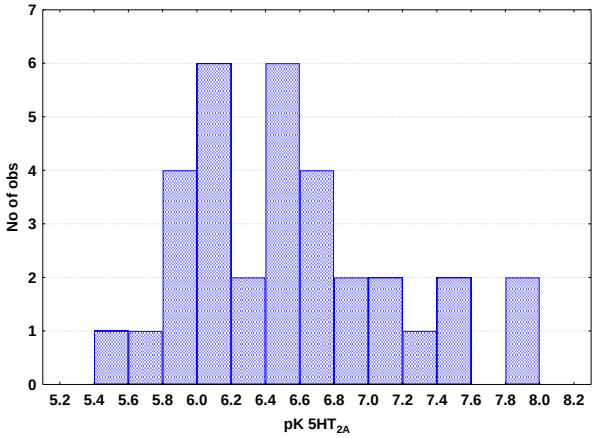

Figure 10: Histogram of frequencies of the data used to obtain Eq. 2.

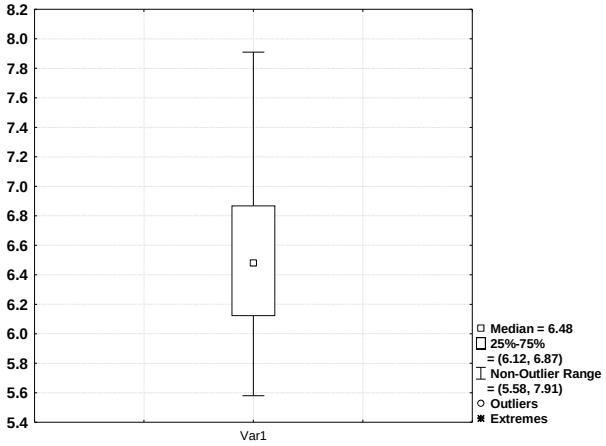

Figure 11: Box-Whiskers plot of values used to obtain Eq. 2.

Figures 12, 13 and 14 show, respectively, the plot of predicted values vs. residuals scores, the plot of residual vs. deleted residuals and the normal probability plot of residuals.

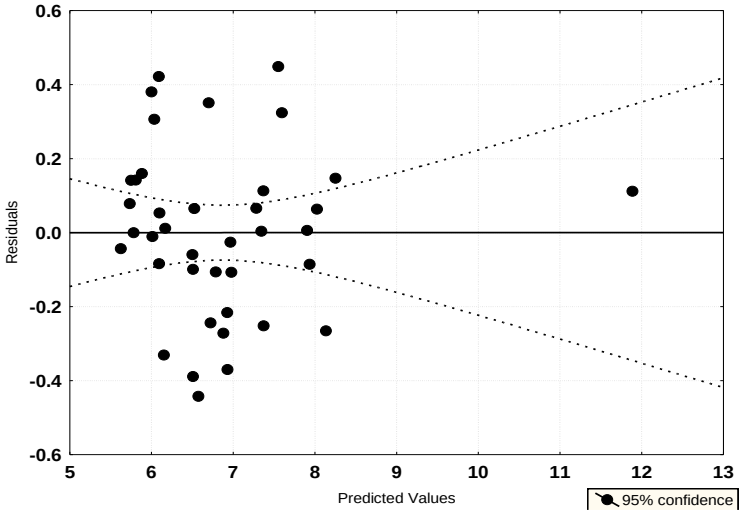

Figure 12: Plot of predicted values vs. residuals scores

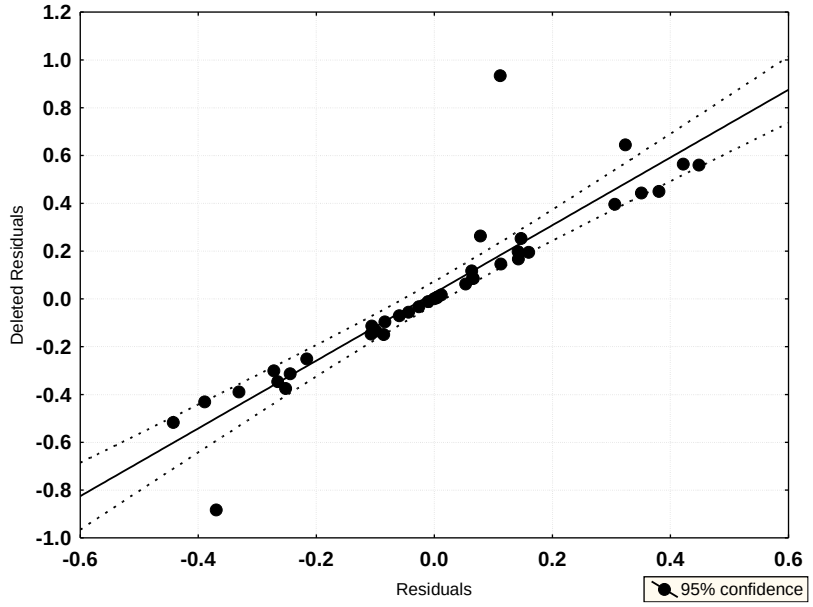

Figure 13: Plot of residuals vs. deleted residuals

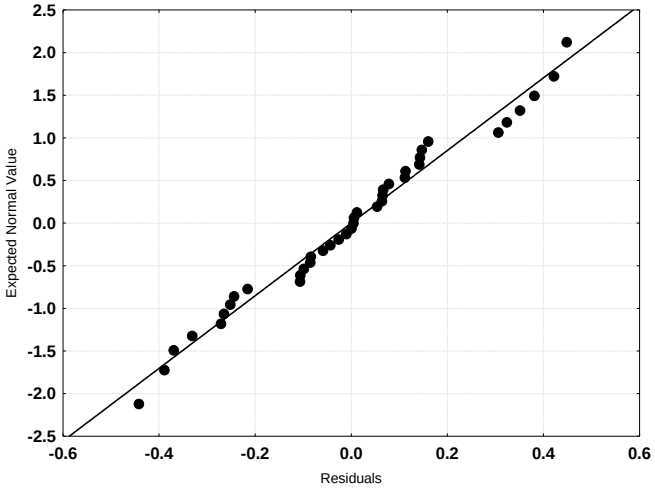

Figure 14: Normal probability plot of residuals

Figures 12 to 14 allow to state that the linear equation 3 is a good approximation to study this biological data and show that the regression coefficients are stable.

Results for the 5-HT$_{2B}$ receptor

The best equation found is:

$$pK_i = 8.06 + 2.19F_{14}(LUMO)^* + 0.06S_{20}^N(LUMO+2)^* - 11.87S_{21}^E(HOMO-1)^* - \\ -1.43S_4^N(LUMO)^* + 0.002S_{23}^N - 18.57s_{13} - 0.10S_6^N(LUMO+1)^* + 0.32S_{22}^N(LUMO)^* + \\ +0.00001S_{22}^N - 0.001S_{21}^N + 0.77S_{13}^E(HOMO-2)^* \quad (3)$$

with n=38, R=0.96, R^2=0.93, adj-R^2=0.89, F(11,26)=29.420 (p<0.00000) and SD=0.16. No outliers were detected, and no residuals fall outside the ±2σ limits. Here, $F_{14}(LUMO)^*$ is the electron population of the lowest empty local MO localized on atom 14, $S_{20}^N(LUMO+2)^*$ is the nucleophilic superdelocalizability of the third lowest empty local

MO of atom 20, S_{21}^{E}(HOMO-1)* is the electrophilic superdelocalizability of the second highest local MO of atom 21, S_{4}^{N}(LUMO)* is the nucleophilic superdelocalizability of the lowest empty local MO of atom 4, S_{23}^{N} is the total atomic nucleophilic superdelocalizability of atom 23, s_{13} is the local atomic softness of atom 13, S_{6}^{N}(LUMO+1)* is the nucleophilic superdelocalizability of the second lowest empty MO of atom 6, S_{22}^{N}(LUMO)* is the nucleophilic superdelocalizability of the lowest empty MO of 22, S_{22}^{N} is the total atomic nucleophilic superdelocalizability of atom 22, S_{21}^{N} is the total atomic nucleophilic superdelocalizability of atom 21, and S_{13}^{E}(HOMO-2)* is the electrophilic superdelocalizability of the third highest occupied local MO of atom 13.

Tables 4 and 5 show the beta coefficients, the results of the t-test for significance of coefficients and the matrix of squared correlation coefficients for the variables of Eq. 3. Figure 15 displays the plot of observed *vs.* calculated pK values.

Table 4: Beta coefficients and t-test for significance of coefficients in Eq. 3.

Variable	Beta	t(26)	p-level
F_{14}(LUMO)*	0.39	5.25	0.00002
S_{20}^{N}(LUMO+2)*	0.31	5.24	0.00002
S_{21}^{E}(HOMO-1)*	-0.40	-6.62	0.000001
S_{4}^{N}(LUMO)*	-0.29	-4.62	0.00009
S_{23}^{N}	0.28	4.78	0.00006
s_{13}	-0.47	-6.09	0.000002
S_{6}^{N}(LUMO+1)*	-0.26	-3.79	0.0008
S_{22}^{N}(LUMO)*	0.27	4.19	0.0003
S_{22}^{N}	0.20	3.47	0.002
S_{21}^{N}	-0.25	-3.78	0.0008
S_{13}^{E}(HOMO-2)*	0.15	2.33	0.03

Table 5: Matrix of squared correlation coefficients for the variables in Eq. 3

	Var268	Var396	Var412	Var74	Var444	Var259	Var115	Var434	Var424	Var404
Var396	**0.08**	**1.00**								
Var412	**0.00**	**0.01**	**1.00**							
Var74	**0.04**	**0.00**	**0.03**	**1.00**						
Var444	**0.01**	**0.02**	**0.00**	**0.02**	**1.00**					
Var259	**0.29**	**0.00**	**0.00**	**0.01**	**0.00**	**1.00**				
Var115	**0.02**	**0.00**	**0.01**	**0.09**	**0.01**	**0.20**	**1.00**			
Var434	**0.00**	**0.02**	**0.11**	**0.08**	**0.02**	**0.00**	**0.06**	**1.00**		
Var424	**0.00**	**0.01**	**0.02**	**0.01**	**0.01**	**0.01**	**0.00**	**0.00**	**1.00**	
Var404	**0.05**	**0.00**	**0.00**	**0.00**	**0.01**	**0.14**	**0.06**	**0.03**	**0.12**	**1.00**
Var251	**0.11**	**0.01**	**0.03**	**0.02**	**0.06**	**0.02**	**0.01**	**0.02**	**0.02**	**0.05**

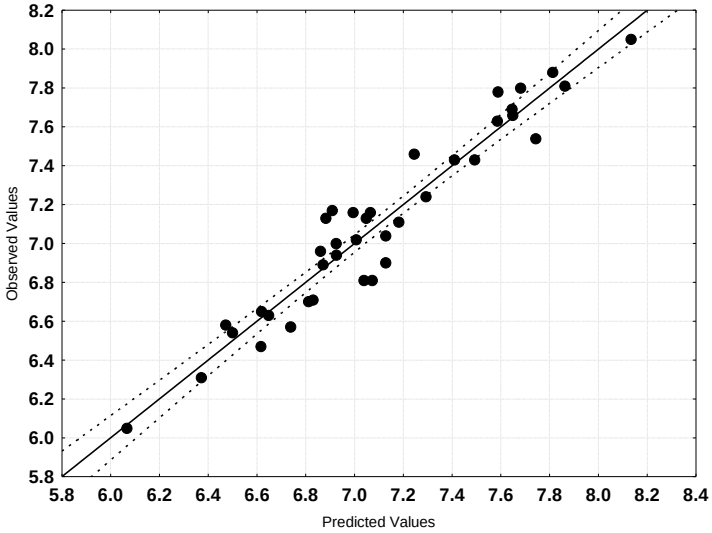

Figure 15: Plot of predicted vs. observed pK_i values (Eq. 3). Dashed lines denote the 95% confidence interval

The associated statistical parameters of Eq. 3 indicate that this equation is statistically significant and that the variation of the numerical values of a group of eleven local atomic reactivity indices of atoms constituting the common skeleton explains about 89% of the variation of the pK values. Figure 15, spanning about 2 orders of magnitude, shows that there is a good correlation of observed *versus* calculated values. Table 4 shows no significant correlations among independent variables. Figures 16, 17 and 18 show, respectively, the plot of predicted values vs. residuals scores, the plot of residual vs. deleted residuals and the normal probability plot of residuals.

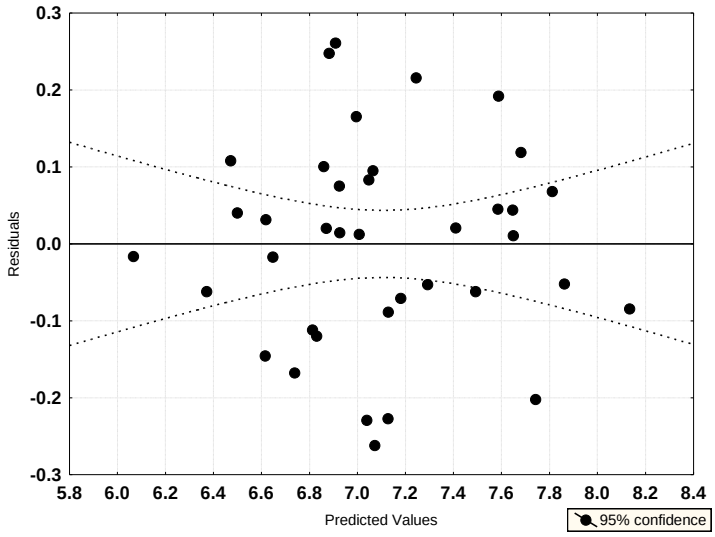

Figure 16: Plot of predicted values vs. residuals scores

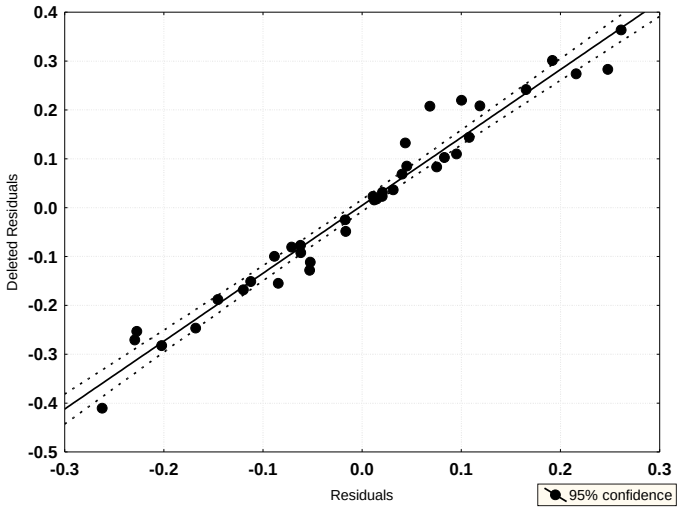

Figure 17: Plot of residuals vs. deleted residuals

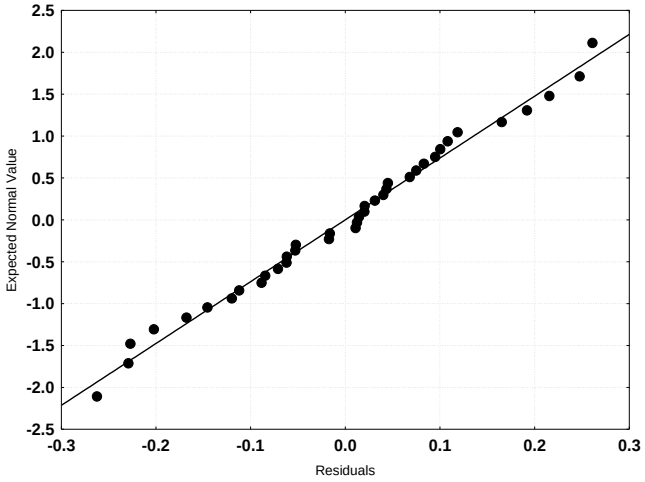

Figure 18: Normal probability plot of residuals

Figures 16 to 18 permit to state that the linear equation 3 is a good approximation to study this biological data and show that the regression coefficients are stable. The next two figures show the histogram of frequencies and the Box-Whiskers plot of values with median and quartile values for the data set (n=38) used to obtain Eq. 3.

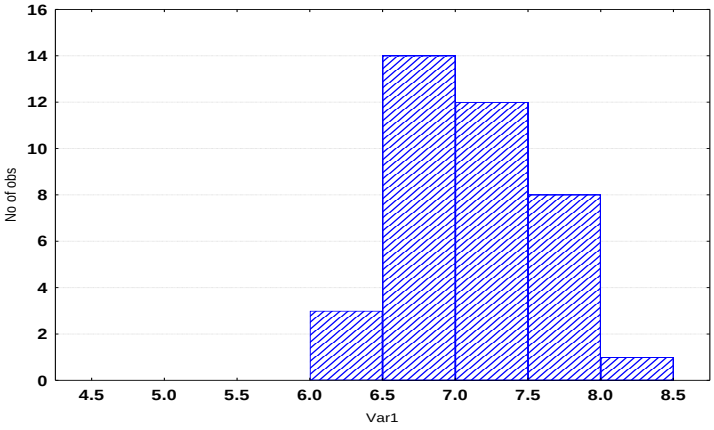

Figure 19: Histogram of frequencies of the data used to obtain Eq. 3.

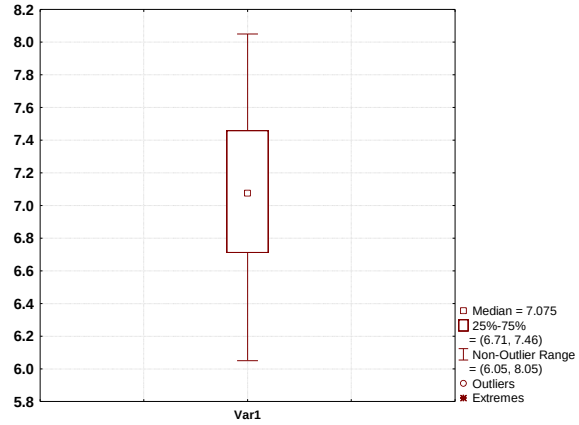

Figure 20: Box-Whiskers plot of values used to obtain Eq. 3.

Results for the 5-HT$_{2C}$ receptor

It was not possible to obtain a single equation for the whole set of data. Therefore, and using an empirical approach we divided the set in two parts. The first set contains the fifteen lowest experimental values and the second one the twenty-six highest experimental values. For both of them we obtained statistically significant QSAR equations.

Results for the 15 lowest experimental values of 5-HT$_{2C}$ receptor affinities

Figures 21 and 22 show, respectively, the histogram of frequencies and the Box-Whiskers plot of values with median and quartile values for the data set (n=15) used to obtain Eq. 4.

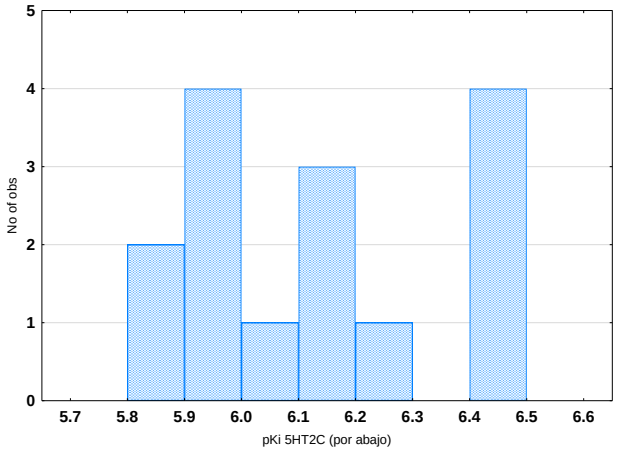

Figure 21: Histogram of frequencies of the data used to obtain Eq. 4.

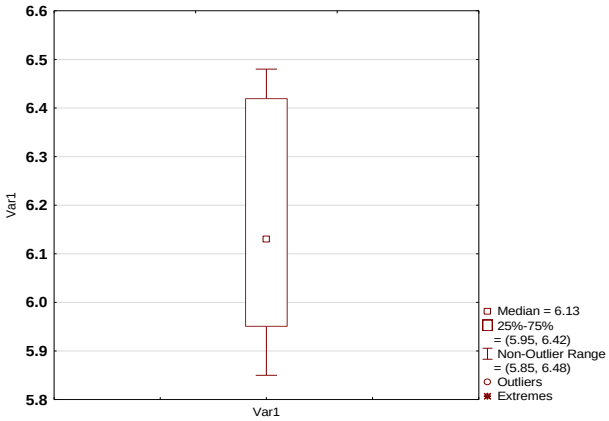

Figure 22: Box-Whiskers plot of values used to obtain Eq. 4

The best equation found is:

$$pK_i = 12.57 - 30.52 s_{16} + 0.99 S_{10}^{N}(LUMO+1)^* - \\ -30.79 F_{10}(LUMO)^* + 0.67 F_{17}(HOMO-2)^* + 0.33 Q_{17} \quad (4)$$

with n=15, R=0.98, R^2=0.96, adj-R^2=0.93, F(5,9)=39.343 (p<0.00001) and SD=0.06. No outliers were detected, and no residuals fall outside the ±2σ limits. Here, s_{16} is the local atomic softness of atom 16, $S_{10}^{N}(LUMO+1)^*$ is the nucleophilic superdelocalizability of the second lowest empty local MO of atom 10, $F_{10}(LUMO)^*$ is the electron population of the lowest empty local MO of atom 10, $F_{17}(HOMO-2)^*$)* is the electron population of the third highest occupied local MO of atom 17, and Q_{17} is the net charge of atom 17.

Table 6: Beta coefficients and t-test for significance of coefficients in Eq. 4.

Variable	Beta	t(9)	p-level
s_{16}	-1.25	-13.76	0.000000
$S_{10}^{N}(LUMO+1)^*$	0.95	9.95	0.000004
$F_{10}(LUMO)^*$	-0.40	-4.86	0.0009
$F_{17}(HOMO-2)^*$	0.42	5.43	0.0004
Q_{17}	0.28	3.74	0.005

Table 7: Matrix of squared correlation coefficients for the variables in Eq. 4.

	s_{16}	$S_{10}^{N}(LUMO+1)^*$	$F_{10}(LUMO)^*$	$F_{17}(HOMO-2)^*$	Q_{17}
s_{16}	1.00				
$S_{10}^{N}(LUMO+1)^*$	0.26	1.00			
$F_{10}(LUMO)^*$	0.00	0.19	1.00		
$F_{17}(HOMO-2)^*$	0.07	0.00	0.03	1.00	
Q_{17}	0.03	0.00	0.00	0.05	1.00

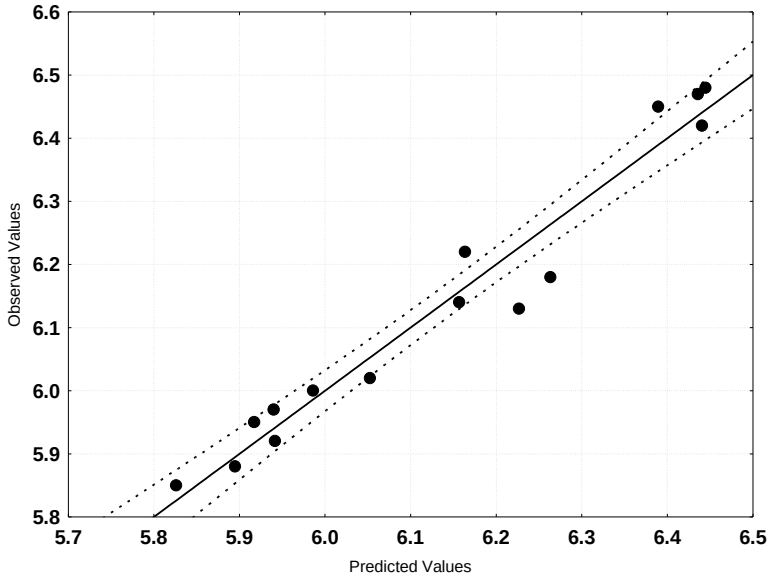

Figure 23: Plot of predicted vs. observed pK_i values (Eq. 4). Dashed lines denote the 95% confidence interval.

The associated statistical parameters of Eq. 4 indicate that this equation is statistically significant and that the variation of the numerical values of a group of five local atomic reactivity indices of atoms constituting the common skeleton explains about 93% of the variation of the pK_i values. Figure 23 shows that there is a good correlation of observed *versus* calculated values. Table 7 shows no significant correlations among independent variables.

Figures 24, 25 and 26 show, respectively, the plot of predicted values vs. residuals scores, the plot of residual vs. deleted residuals and the normal probability plot of residuals.

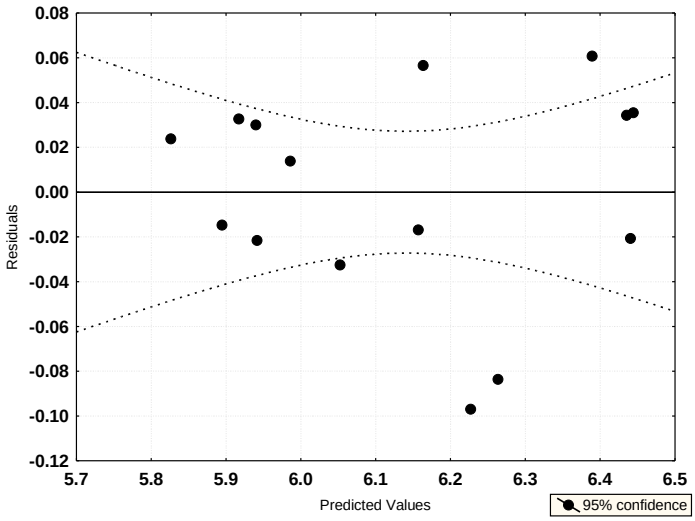

Figure 24: Plot of predicted values vs. residuals scores

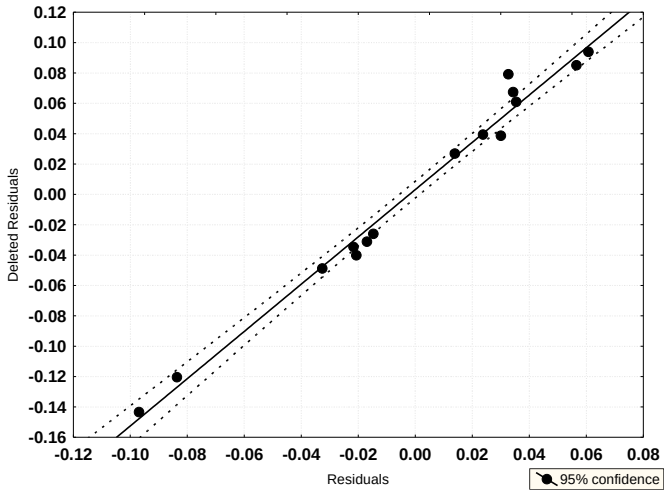

Figure 25: Plot of residuals vs. deleted residuals

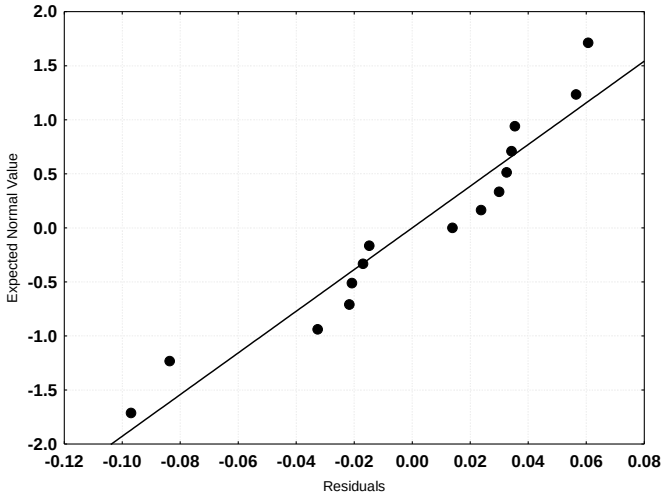

Figure 26: Normal probability plot of residuals

Figures 24 to 26 allow to state that the linear equation 3 is a good approximation to study this biological data and show that the regression coefficients are stable.

Results for the 26 highest experimental values of 5-HT$_{2C}$ receptor affinities

Figures 27 and 28 show, respectively, the histogram of frequencies and the Box-Whiskers plot of values with median and quartile values for the data set (n=26) used to obtain Eq. 5.

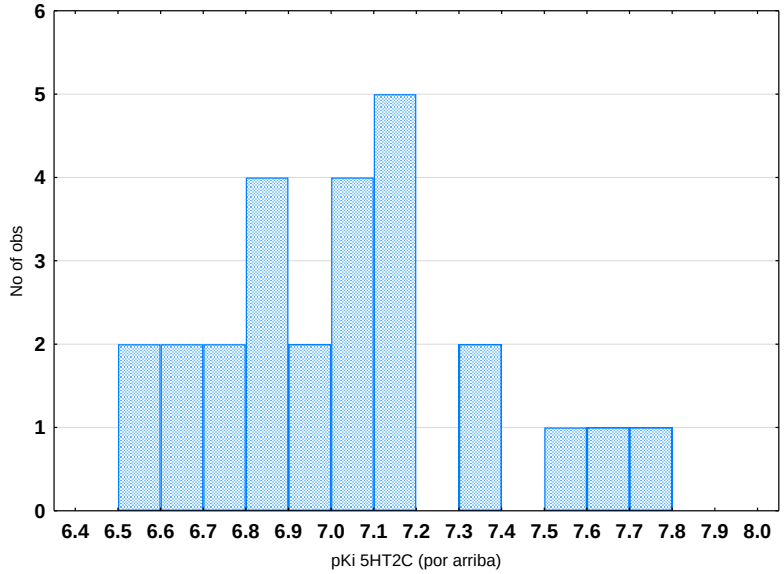

Figure 27: Histogram of frequencies of the data used to obtain Eq. 5

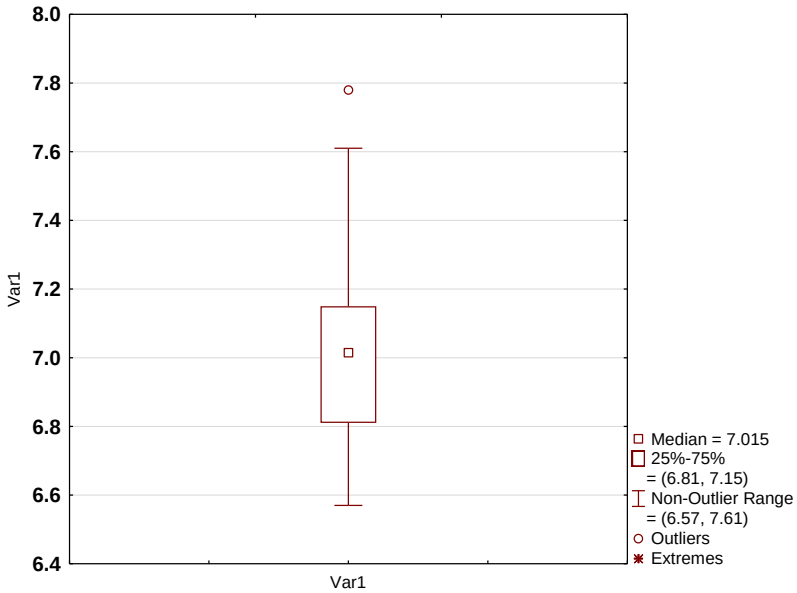

Figure 28: Box-Whiskers plot of values used to obtain Eq. 5

The best equation found is:

$$pK_i = 7.90 + 1.81F_8(\text{LUMO}+1)^* - 2.80F_6(\text{HOMO}-2)^* + \\ + 0.22S_{18}^E(\text{HOMO}-1)^* + 1.27S_{13}^E(\text{HOMO}-1)^* - 0.08S_4^N(\text{LUMO}+2)^* + \\ + 0.003S_6^N + 0.65F_5(\text{LUMO})^* \quad (5)$$

with n=26, R=0.98, R^2=0.95, adj-R^2=0.93, F(7,18)=51.080 (p<0.00000) and SD=0.08. No outliers were detected, and no residuals fall outside the ±2σ limits. Here, F_8(LUMO+1)* is the electron population of the second lowest empty local MO of atom 8, F_6(HOMO-2)* is the electron population of the third highest occupied local MO of atom 6, S_{18}^E(HOMO-1)* is the electrophilic superdelocalizability of the second highest occupied local MO of atom 18, S_{13}^E(HOMO-1)* is the electrophilic superdelocalizability of the second highest occupied local MO of atom 13, S_6^N is the total atomic nucleophilic superdelocalizability of atom 6, and F_5(LUMO)* is the electron population of the lowest empty local MO of atom 5.

Table 8: Beta coefficients and t-test for significance of coefficients in Eq. 5.

Variable	Beta	t(18)	p-level
F_8(LUMO+1)*	0.63	11.47	0.000000
F_6(HOMO-2)*	-0.19	-2.87	0.01
S_{18}^E(HOMO-1)*	0.39	7.10	0.000001
S_{13}^E(HOMO-1)*	0.38	6.71	0.000003
S_4^N(LUMO+2)*	-0.27	-4.90	0.0001
S_6^N	0.34	4.90	0.0001
F_5(LUMO)*	0.19	3.24	0.005

Table 9: Matrix of squared correlation coefficients for the variables in Eq. 5.

	Var149	Var105	Var352	Var252	Var76	Var104
Var149	1.00					
Var105	0.00	1.00				
Var352	0.01	0.05	1.00			
Var252	0.02	0.01	0.00	1.00		
Var76	0.02	0.02	0.01	0.09	1.00	
Var104	0.02	0.29	0.00	0.05	0.03	1.00
Var88	0.03	0.03	0.03	0.02	0.03	0.07

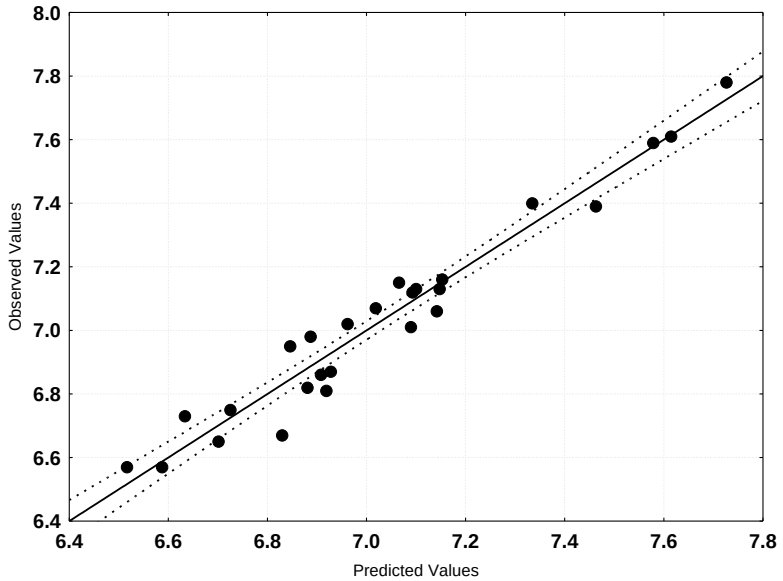

Figure 29: Plot of predicted vs. observed pK_i values (Eq. 5). Dashed lines denote the 95% confidence interval.

The associated statistical parameters of Eq. 5 indicate that this equation is statistically significant and that the variation of the numerical values of a group of seven local atomic reactivity indices of atoms constituting the common skeleton explains about 93% of the variation of the receptor affinity. Figure 29 shows that there is a good

correlation of observed *versus* calculated values. Table 9 shows no significant correlations among independent variables.

Figures 30, 31 and 32 show, respectively, the plot of predicted values vs. residuals scores, the plot of residual vs. deleted residuals and the normal probability plot of residuals.

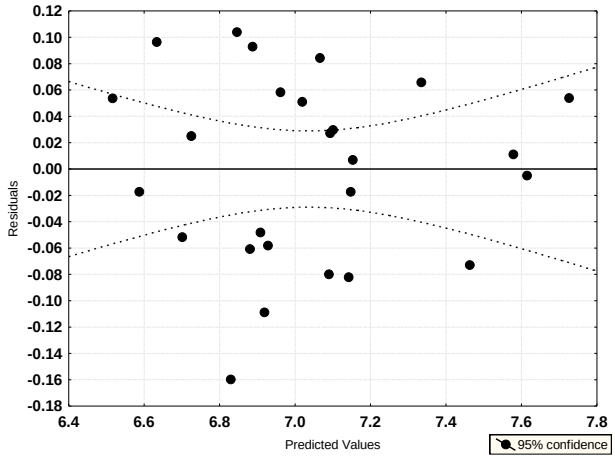

Figure 30: Plot of predicted values vs. residuals scores

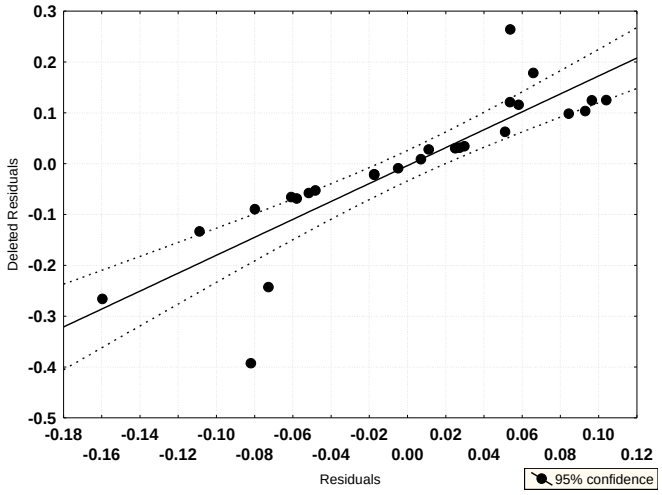

Figure 31: Plot of residuals vs. deleted residuals

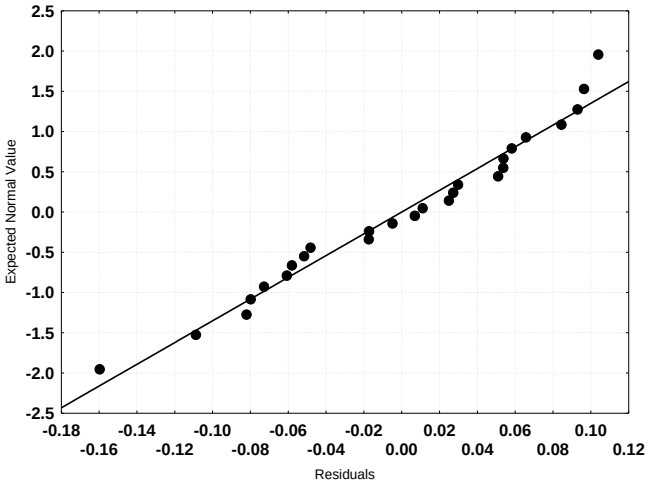

Figure 32: Normal probability plot of residuals

Figures 30 to 32 allow us to state that the linear equation 3 is a good approximation to study this biological data and show that the regression coefficients are stable.

Local Molecular Orbitals.

Tables 10 to 13 show the Local Molecular Orbitals of atoms appearing in the QSAR equations.

Table 10. Local Molecular Orbitals of atoms 4, 5, and 6.

Mol.	Atom 4 (sp^2 C)	Atom 5 (sp^2 C)	Atom 6 (sp^2 C)
1 (67)	65π66π67π-71π73π74π	65π66π67π-71π72π73π	65π66π67π-71π73π74π
2 (71)	68π70π71π-74π77π78π	68π70π71π-74π76π77π	68π70π71π-74π77π78π
3 (75)	72π74π75π-78π80π81π	72π74π75π-78π80π82π	72π74π75π-78π80π81π
4 (71)	69π70π71π-75π77π78π	68π70π71π-75π77π78π	69π70π71π-75π77π78π
5 (75)	73π74π75π-79π81π82π	73π74π75π-79π81π82π	73π74π75π-78π79π81π
6 (84)	82π83π84π-88π90π91π	82π83π84π-88π90π91π	82π83π84π-88π90π92π
7 (71)	68π70π71π-75π77π78π	68π70π71π-75π76π77π	68π70π71π-75π77π78π
8 (71)	68π70π71π-75π77π78π	68π70π71π-75π76π77π	68π70π71π-75π77π78π
9 (71)	69π70π71π-75π77π78π	69π70π71π-75π76π77π	69π70π71π-75π77π78π
10 (75)	72π74π75π-79π82π83π	72π74π75π-79π81π82π	72π74π75π-79π82π83π
11 (84)	81π83π84π-88π91π92π	81π83π84π-88π90π91π	81π83π84π-88π91π92π
12 (71)	68π70π71π-75π77π78π	68π70π71π-75π76π77π	68π70π71π-75π77π78π
13 (75)	72π74π75π-79π81π82π	72π74π75π-79π80π81π	72π74π75π-78π79π80π
14 (71)	69π70π71π-75π77π78π	69π70π71π-75π76π77π	69π70π71π-75π77π78π
15 (79)	76π78π79π-83π84π85π	76π78π79π-83π84π85π	76π78π79π-82π83π84π
16 (75)	73π74π75π-79π82π83π	72π74π75π-79π81 82π	73π74π75π-79π82π83π
17 (84)	81π83π84π-88π91π92π	81π83π84π-88π90π91π	81π83π84π-88π91π92π
18 (78)	76π77π78π-83π85π86π	76π77π78π-83π85π86π	76π77π78π-83π85π86π
19 (79)	76π78π79π-82π84π85π	76π78π79π-82π84π86π	76π78π79π-82π84π86π
20 (83)	80π82π83π-86π88π89π	80π82π83π-86π88π90π	80π82π83π-86π88π90π
21 (88)	85π87π88π-92π94π95π	85π87π88π-92π94π95π	85π87π88π-92π94π96π
22 (75)	72π74π75π-78π81π82π	72π74π75π-78π80π81π	72π74π75π-78π81π82π
23 (75)	72π74π75π-78π80π81π	72π74π75π-78π80π81π	72π74π75π-78π81π82π

24 (75)	72π74π75π-78π81π82π	72π74π75π-78π81π82π	72π74π75π-78π81π82π
25 (79)	76π78π79π-83π85π86π	76π78π79π-83π84π85π	76π78π79π-83π85π86π
26 (88)	85π87π88π-91π95π96π	85π87π88π-91π95π96π	85π87π88π-91π95π96π
27 (92)	89π91π92π-95π98π99π	89π91π92π-95π98π100π	89π91π92π-95π98π100π
28 (83)	80π82π83π-86π89π90π	80π82π83π-86π89π91π	80π82π83π-86π89π90π
29 (83)	80π82π83π-86π88π89π	80π82π83π-86π88π90π	80π82π83π-86π88π89π
30 (82)	80π81π82π-86π89π90π	80π81π82π-86π89π90π	80π81π82π-86π87π89π
31 (88)	85π87π88π-91π95π96π	85π87π88π-91π94π95π	85π87π88π-91π95π96π
32 (83)	79π82π83π-86π88π89π	79π82π83π-86π88π90π	79π82π83π-86π88π89π
33 (88)	85π87π88π-92π94π95π	85π87π88π-92π94π97π	85π87π88π-92π94π96π
34 (75)	72π74π75π-78π81π82π	72π74π75π-78π80π81π	72π74π75π-78π81π82π
35 (105)	102π104π105π-109π112π113π	102π104π105π-109π112π113π	102π104π105π-109π110π112π
36 (83)	79π82π83π-87π88π89π	79π82π83π-87π88π89π	79π82π83π-86π87π88π
37 (75)	73π74π75π-79π81π82π	73π74π75π-81π82π83π	73π74π75π-79π82π84π
38 (83)	80π82π83π-86π89π90π	80π82π83π-88π89π90π	80π82π83π-86π89π90π
39 (83)	80π82π83π-87π90π91π	80π82π83π-90π91π92π	80π82π83π-87π90π91π
40 (92)	89π91π92π-97π99π100π	89π91π92π-99π100π101π	89π91π92π-97π99π100π
41 (92)	89π91π92π-96π99π100π	89π91π92π-99π100π101π	89π91π92π-96π100π102π
42 (87)	84π86π87π-90π93π94π	84π86π87π-93π94π95π	84π86π87π-90π93π94π
43 (83)	80π82π83π-86π87π89π	80π82π83π-89π90π91π	80π82π83π-86π87π90π

Table 11: Local Molecular Orbitals of atoms 8, 9, 10, and 13.

Mol.	Atom 8 (sp^2 C)	Atom 9 (sp^2 N)	Atom 10 (sp^3 C)	Atom 13 (sp^3 C)
1 (67)	65π66π67π-71π72π73π	65π66π67π-71π72π73π	61σ65σ67σ-70σ75σ78σ	56σ58σ63σ-68σ70σ76σ
2 (71)	68π70π71π-74π77π78π	68π70π71π-74π76π77π	65σ68σ71σ-75σ78σ80σ	62σ63σ67σ-72σ73σ75σ
3 (75)	72π74π75π-78π80π81π	72π74π75π-78π80π82π	69σ72σ75σ-79σ81σ85σ	64σ66σ71σ-76σ77σ79σ
4 (71)	68π70π71π-74π75π77π	69π70π71π-75π77π78π	65σ68σ71σ-74σ79σ81σ	62σ63σ67σ-72σ80σ81σ
5 (75)	73π74π75π-78π79π80π	73π74π75π-79π81π83π	69σ73σ75σ-80σ82σ84σ	64σ67σ71σ-76σ78σ80σ

6 (84)	82π83π84π- 88π90π92π	82π83π84π- 88π90π92π	78σ82σ84σ- 89σ91σ93σ	73σ77σ80σ- 85σ87σ89σ
7 (71)	68π70π71π- 74π75π76π	68π70π71π- 75π76π77π	65σ68σ71σ- 74σ79σ82σ	62σ63σ67σ- 72σ73σ80σ
8 (71)	68π70π71π- 75π76π77π	68π70π71π- 75π76π77π	65σ68σ71σ- 74σ79σ81σ	62σ63σ67σ- 72σ74σ80σ
9 (71)	69π70π71π- 75π77π78π	69π70π71π- 75π77π78π	65σ69σ71σ- 74σ79σ82σ	61σ63σ67σ- 72σ73σ74σ
10 (75)	72π74π75π- 79π82π83π	72π74π75π- 79π82π83π	68σ72σ75σ- 78σ84σ86σ	63σ64σ71σ- 76σ78σ80σ
11 (84)	81π83π84π- 88π91π92π	81π83π84π- 88π91π92π	77σ81σ84σ- 87σ93σ95σ	72σ74σ79σ- 85σ87σ89σ
12 (71)	68π70π71π- 74π75π76π	68π70π71π- 75π76π77π	65σ68σ71σ- 74σ79σ82σ	60σ63σ69σ- 72σ80σ81σ
13 (75)	72π74π75π- 78π79π80π	72π74π75π- 79π80π81π	69σ72σ75σ- 78σ82σ83σ	65σ67σ73σ- 76σ77σ84σ
14 (71)	69π70π71π- 74π75π76π	69π70π71π- 75π76π77π	65σ68σ71σ- 74σ79σ81σ	61σ62σ69σ- 72σ80σ81σ
15 (79)	76π78π79π- 82π83π84π	76π78π79π- 83π84π85π	73σ76σ79σ- 82σ86σ87σ	65σ67σ77σ- 80σ81σ88σ
16 (75)	72π74π75π- 79π82π83π	73π74π75π- 79π82π83π	68σ72σ75σ- 78σ84σ86σ	64σ66σ73σ- 76σ78σ80σ
17 (84)	81π83π84π- 88π91π92π	81π83π84π- 88π91π92π	77σ81σ84σ- 87σ93σ95σ	72σ74σ82σ- 85σ87σ89σ
18 (78)	76π77π78π- 82π83π85π	76π77π78π- 83π85π86π	69σ76σ78σ- 82σ87σ89σ	65σ66σ72σ- 79σ81σ88σ
19 (79)	76π78π79π- 82π84π86π	76π78π79π- 82π84π86π	73σ76σ79σ- 83σ85σ86σ	70σ71σ75σ- 80σ83σ87σ
20 (83)	80π82π83π- 86π88π89π	80π82π83π- 86π88π90π	76σ80σ83σ- 87σ89σ93σ	75σ78σ79σ- 84σ87σ91σ
21 (88)	85π87π88π- 92π94π95π	85π87π88π- 92π94π96π	81σ85σ88σ- 93σ95σ98σ	76σ77σ84σ- 89σ90σ91σ
22 (75)	72π74π75π- 78π81π82π	72π74π75π- 78π81π82π	69σ72σ75σ- 79σ82σ84σ	63σ65σ71σ- 76σ77σ79σ
23 (75)	72π74π75π- 78π80π81π	72π74π75π- 78π80π81π	69σ72σ75σ- 79σ82σ84σ	65σ66σ71σ- 76σ77σ79σ
24 (75)	72π74π75π- 78π81π82π	72π74π75π- 78π81π82π	69σ72σ75σ- 79σ82σ83σ	64σ66σ71σ- 76σ77σ82σ
25 (79)	76π78π79π- 83π84π85π	76π78π79π- 83π85π86π	73σ76σ79σ- 81σ84σ87σ	69σ70σ75σ- 80σ81σ82σ
26 (88)	85π87π88π- 91π95π96π	85π87π88π- 91π95π96π	80σ85σ88σ- 92σ96σ98σ	76σ77σ83σ- 89σ90σ92σ
27 (92)	89π91π92π- 95π98π100π	89π91π92π- 95π98π100π	84σ89σ92σ- 96σ99σ101σ	81σ82σ87σ- 93σ94σ96σ
28 (83)	80π82π83π- 86π89π90π	80π82π83π- 86π89π91π	75σ80σ83σ- 87σ90σ92σ	71σ73σ79σ- 84σ85σ87σ
29 (83)	80π82π83π- 86π88π89π	80π82π83π- 86π88π90π	76σ80σ83σ- 87σ89σ94σ	73σ75σ79σ- 84σ85σ92σ
30 (82)	80π81π82π- 86π89π90π	80π81π82π- 86π89π90π	73σ80σ82σ- 87σ90σ92σ	69σ70σ75σ- 83σ84σ85σ
31 (88)	85π87π88π- 91π95π96π	85π87π88π- 91π95π96π	80σ85σ88σ- 92σ96σ98σ	78σ81σ86σ- 89σ90σ92σ
32 (83)	79π82π83π- 86π88π89π	79π82π83π- 86π88π90π	76σ79σ83σ- 87σ89σ94σ	72σ73σ81σ- 84σ85σ93σ
33 (88)	85π87π88π-	85π87π88π-	82σ85σ88σ-	77σ81σ84σ-

	92π94π96π	92π94π97π	93σ97σ100σ	89σ90σ91σ
34 (75)	72π74π75π-78π81π82π	72π74π75π-78π81π82π	69σ72σ75σ-79σ82σ83σ	64σ65σ71σ-76σ79σ83σ
35 (105)	102π104π105π-109π110π112π	102π104π105π-109π112π114π	96σ102σ105σ-110σ114σ116σ	91σ92σ99σ-106σ107σ108σ
36 (83)	79π82π83π-86π87π88π	79π82π83π-87π88π89π	76σ79σ83σ-86σ89σ90σ	72σ74σ81σ-84σ85σ92σ
37 (75)	73π74π75π-79π82π83π	73π74π75π-79π81π82π	69σ73σ74σ-78σ80σ81σ	61σ65σ70σ-76σ78σ84σ
38 (83)	80π82π83π-86π90π91π	80π82π83π-86π89π90π	77σ80σ82σ-87σ88σ89σ	70σ73σ78σ-84σ85σ87σ
39 (83)	80π82π83π-87π90π91π	80π82π83π-87π91π92π	77σ80σ82σ-86σ89σ90σ	69σ76σ78σ-84σ86σ88σ
40 (92)	89π91π92π-97π99π100π	89π91π92π-97π100π101π	85σ89σ91σ-95σ98σ99σ	81σ86σ87σ-93σ95σ96σ
41 (92)	89π91π92π-96π99π100π	89π91π92π-96π99π100π	85σ89σ91σ-95σ99σ101σ	81σ84σ90σ-93σ95σ97σ
42 (87)	84π86π87π-90π94π95π	84π86π87π-90π93π94π	81σ84σ86σ-91σ93σ94σ	74σ78σ82σ-88σ89σ95σ
43 (83)	80π82π83π-86π87π90π	80π82π83π-86π89π90π	77σ80σ82σ-87σ89σ91σ	68σ73σ78σ-84σ85σ87σ

Table 12. Local Molecular Orbitals of atoms 14, 16, 17, and 18.

Mol.	Atom 14 (sp^2 C)	Atom 16 (sp^2 C)	Atom 17 (sp^2 C)	Atom 18 (sp^2 C)
1 (67)	59σ63π65π-68π70π74π	59σ63π64-68π69π70π	59σ63π65π-68π69π70π	59σ63π64-68π69π70π
2 (71)	63π67π69π-72π73π75π	63π67π69π-72π73π76σ	63π67π69π-72π73π75π	62 63π69π-72π73π75π
3 (75)	67π71π73π-76π77π79π	67π71π73π-76π77π82π	67π71π73π-76π77π79π	66 67π73π-76π77π79π
4 (71)	63σ67π69π-72π73π74π	67π68π69π-72π73π78π	63σ67π69π-72π73π74π	67π68π69π-72π73π74π
5 (75)	67σ71π72π-76π77π78σ	67σ71π72π-76π77π78σ	67σ71π72π-76π77π78σ	67σ71π72π-76π77 80π
6 (84)	77σ80π81π-85π86π87σ	77σ80π81π-85π86π87σ	77σ80π81π-85π86π87σ	75π80π81π-85π86π89π
7 (71)	63π67π69π-72π74π78?	62σ63σ69π-72π73π74π	63? 67π69π-72π73π74π	63π67π69π-72π73π76π
8 (71)	63σ67π69π-72π74π78 σ	63σ68π69π-72π73π74π	63σ67π69π-72π73π74π	67π68π69π-72π73π74π
9 (71)	67π68π69π-72π73π74π	63σ67π68π-72π73π76π	67π68π69π-72π73π74π	67π68π69π-72π73π74π
10 (75)	70σ71π73π-76π78π80σ	70σ71π73π-76π77π80σ	70σ71π73π-76π77π78π	66π70σ73π-76π77π78π
11 (84)	77π79π82π-85π87π89σ	79π80σ82π-85π86π87π	79π80σ82π-85π86π87π	77π80σ82π-85π86π87π
12 (71)	62π63σ69π-72π73π74π	63σ67π69π-72π73π74π	62σ63σ69π-72π73π74π	63σ67π69π-72π73π76π
13 (75)	68σ71π73π-76π77π78π	68 σ71π73π-76π77π78π	67π68 σπ73π-76π77π78π	68 σ71π73π-76π77π78π
14 (71)	63σ68π69π-72π74π78σ	67π68π69π-72π73π74π	63σ68π69π-72π73π74π	67π68π69π-72π73π74π

15 (79)	73π75π77π- 80π81π82π	71σ75π77π- 80π81π82π	72π73π77π- 80π81π82π	71σ75π77π- 80π81π82π
16 (75)	66π72π73π- 76π78π83π	71π72π73π- 76π77π78π	70σ72π73π- 76π77π78π	71π72π73π- 76π77π78π
17 (84)	76π77π82π- 85π87π92π	79π80σ82π- 85π86π87π	77π80σ82π- 85π86π87π	79π80σ82π- 85π86π87π
18 (78)	65σ66σ72π- 79π80π81π	73σ74π75σ- 79π80π86?	66σ72π73σ- 79π80π81π	73σ74π75σ- 79π80π86?
19 (79)	75π76π77π- 80π81π83π	75π76π77π- 80π81π83π	75π76π77π- 80π81π83π	75π76π77π- 80π81π83π
20 (83)	78σ79π80π- 84π85π87π	79π80π81π- 84π85π87π	79π80π81π- 84π85π87π	79π80π81π- 84π85π87π
21 (88)	80π84π86π- 89π90π91σ	83σ84π86π- 89π90π91σ	77σ83σ84π- 89π90π91σ	83σ84π86π- 89π90π91σ
22 (75)	67π71π73π- 76π77π79π	67π71π73π- 76π77π79π	65σ67π71π- 76π77π79π	67π71π73π- 76π77π79π
23 (75)	67π71π73π- 76π77π79π	66σ67π73π- 76π77π79π	67π71π73π- 76π77π79π	67π71π73π- 76π77π80σ
24 (75)	67π71π73π- 76π77π79π	67π71π73π- 76π77π80σ	67π71π73π- 76π77π79π	66σ67π73π- 76π77π79π
25 (79)	72π75π77π- 80π82π87σ	72π75π77π- 80π82π84π	72π75π77π- 80π82π90σ	70σ72π77π- 80π82π84π
26 (88)	82π83π86π- 89π90π92π	82π84 86π- 89π90π91σ	83π84 86π- 89π90π92π	82π83π86π- 89π90π92π
27 (92)	86π87π90π- 93π94π96π	86π87π90π- 93π94π97σ	87π88σ90π- 93π94π96π	86π88σ90π- 93π94π96π
28 (83)	78σ79π81π- 84π85π87π	78σ79π81π- 84π85π88σ	78σ79π81π- 84π85π87π	76π78σ81π- 84π85π87π
29 (83)	78π79π81π- 84π87π90π	75σ78π81π- 84π85π87π	78π79π81π- 84π85π87π	78π79π81π- 84π85π87π
30 (82)	75π77π79π- 83π84π87π	70π76 σ79π- 83π84π85π	77π78σ79π- 83π84π85π	75π77π79π- 83π84π85π
31 (88)	81π82π86π- 89π90π92π	83σ84σ86π- 89π90π92π	83σ84σ86π- 89π90π92σ	83σ84σ86π- 89π90π92σ
32 (83)	78π80π81π- 84π85π87π	78π80π81π- 84π85π87π	78π80π81π- 84π85π87π	75σ80π81π- 84π85π90π
33 (88)	81σ84π86π- 89π90π91π	81σ84π86π- 89π90π91π	81σ84π86π- 89π90π91π	81π84π86π- 89π90π91π
34 (75)	67π71π73π- 76π77π79π	67π71π73π- 76π77π79π	67π71π73π- 76π77π79π	71π72π73π- 76π77π79π
35 (105)	99π101π103π- 106π107π108σ	98σ101π103π- 106π107π108σ	100σ101π103π- 106π107π108σ	100σ101π103π- 106π107π108σ
36 (83)	78π80π81πσ- 84π86π87π	78π80π81π- 84π85π88π	78σ80π81π- 84π85π86π	78σ80π81π- 84π85π86π
37 (75)	65σ66σ70π- 76π78π81	66σ70π72 σ- 76π77π78π	66σ70π71σ- 76π77π78π	66σ70π72σ- 76π77π78π
38 (83)	74π78π81π- 84π85π87π	74π78π81π- 84π85π88π	74π78π81π- 84π85π87π	73σ74π81π- 84π85π87π
39 (83)	76σ78π81π- 84π85π88σ	76σ78π81π- 84π85π88σ	76σ78π81π- 84π85π88σ	73π78π81π- 84π85π95π
40 (92)	86σ87π90π- 93π94π96σ	86σ87π90π- 93π94π96σ	86σ87π90π- 93π94π96σ	84π87π90π- 93π94π105π
41 (92)	81σ84π90π- 93π95π99π	86π87σ90π- 93π94π95π	84π87σ90π- 93π94π95π	86π87σ90π- 93π94π95π
42 (87)	80π82π85π-	80π82π85π-	80π82π85π-	78σ80π85π-

	88π91π94π	88π89π91π	88π89π91π	88π89π91π
43 (83)	74π78π81π- 84π85π87π	74π78π81π- 84π85π88	74π78π81π- 84π85π87π	73σ74π81π- 84π85π87π

Table 13. Local Molecular Orbitals of atoms 20, 21, and 22.

Mol.	Atom 20 (H)	Atom 21 (H)	Atom 22 (H)
1 (67)	44σ49σ51σ- 68σ69σ70σ	43σ48σ49σ– 68σ69σ70σ	51σ52σ61σ- 76σ78σ79σ
2 (71)	47σ53σ55σ- 72σ73σ75σ	49σ51σ55σ- 72σ73σ75σ	55σ56σ65σ- 79σ81σ83σ
3 (75)	52σ55σ57σ- 76σ77σ79σ	52σ54σ56σ- 76σ77σ79σ	57σ58σ69σ- 84σ85σ86 σ
4 (71)	43σ45σ50σ- 72σ73σ74σ	45σ49σ51σ- 72σ73σ74σ	54σ55σ65σ- 80σ83σ84σ
5 (75)	49σ52σ55σ- 76σ80σ81σ	54σ56σ58σ- 76σ78σ80σ	57σ59σ69σ- 85σ88σ89σ
6 (84)	65σ75σ77σ- 85σ87σ89σ	61σ62σ65σ- 85σ88σ89σ	66σ67σ78σ- 94σ97σ98σ
7 (71)	48σ51σ53σ- 72σ74σ76σ	46σ50σ52σ- 72σ73σ74σ	53σ55σ65 σ- 81σ83σ84σ
8 (71)	49σ50σ52σ- 72σ73σ74σ	45σ47σ49σ- 72σ73σ74σ	52σ55σ65σ- 80σ82σ83σ
9 (71)	46σ50σ54σ- 72σ73σ74σ	50σ52σ53σ- 72σ74σ76σ	54σ55σ65σ- 80σ84σ85σ
10 (75)	50σ53σ57σ- 76σ77σ78σ	53σ54σ56σ- 76σ77σ78σ	57σ58σ68σ- 85σ88σ89σ
11 (84)	59σ62σ66σ- 85σ86σ87σ	59σ63σ64σ- 85σ86σ87σ	60σ66σ67σ- 94σ97σ98σ
12 (71)	45σ50σ53σ- 72σ73σ74σ	46σ48σ52σ- 72σ73σ74σ	53σ55σ65σ- 81σ83σ84σ
13 (75)	48σ53σ56σ- 76σ77σ78σ	48σ53σ55σ- 76σ77σ78σ	56 σ57σ69σ- 84σ86σ87σ
14 (71)	43σ45σ49σ- 72σ73σ74σ	45σ49σ51σ- 72σ73σ74σ	53σ55σ65σ- 80σ83σ84σ
15 (79)	50σ55σ58σ- 80σ81σ82σ	50σ55σ57σ- 80σ81σ82σ	58σ59σ72σ- 88σ90σ91σ
16 (75)	53σ54σ57σ- 76σ77σ78σ	54σ55σ56σ- 76σ77σ78σ	57σ58σ68σ- 85σ88σ89σ
17 (84)	62σ63σ66σ- 85σ86σ87σ	62σ63σ64σ- 85σ86σ87σ	65σ66σ67σ- 94σ98σ99σ
18 (78)	51σ52σ57σ- 79σ80σ81σ	52σ57σ58σ- 80σ81σ82σ	59σ61σ69σ- 88σ92σ93σ
19 (79)	50σ54σ59σ- 80σ83σ84σ	56σ57σ61σ- 80σ83σ85σ	60σ62σ73σ- 87σ88σ89σ
20 (83)	57σ58σ61σ- 84σ87σ89σ	60σ61σ63σ- 84σ87σ89σ	62σ64σ76σ- 92σ93σ94 σ
21 (88)	62σ68σ70σ- 89σ90σ91σ	64σ69σ70σ- 89σ90σ91σ	70σ71σ81σ- 98σ99σ101σ
22 (75)	52σ57σ59σ- 76σ79σ80σ	53σ55σ59σ- 76σ79σ80σ	59σ60σ69σ- 87σ88σ89σ
23 (75)	48σ50σ55σ- 76σ77σ79σ	53σ54σ57σ- 76σ77σ79σ	57σ58σ69σ- 83σ85σ87σ
24 (75)	49σ55σ58σ- 76σ77σ79σ	53σ55σ57σ- 76σ77σ78σ	59σ60σ69σ- 85σ86σ88σ
25 (79)	54σ56σ60σ-	54σ57σ59σ-	60σ62σ73σ-

	81σ82σ84σ	81σ82σ84σ	88σ91σ92 σ
26 (88)	64σ68σ70σ- 89σ90σ92σ	67σ69σ70σ- 89σ90σ92σ	70σ71σ80σ- 99σ101σ102σ
27 (92)	67σ70σ71σ- 93σ94σ96σ	67σ69σ70σ- 93σ94σ96σ	72σ73σ84σ- 102σ103σ105σ
28 (83)	58σ61σ62σ- 84σ85σ87σ	60σ61σ62σ- 84σ85σ87σ	63σ64σ75σ- 93σ94σ96σ
29 (83)	57σ59σ61σ- 84σ85σ87σ	54σ60σ61σ– 84σ85σ87σ	62σ64σ76σ- 92σ93σ94σ
30 (82)	58σ61σ64σ- 84σ85σ86σ	55σ61σ62σ- 84σ85σ86σ	64σ65σ73σ- 93σ96σ97σ
31 (88)	66σ67σ70σ- 89σ90σ92σ	62σ66σ69σ- 89σ90σ92σ	70σ71σ80σ- 99σ101σ102σ
32 (83)	59σ60σ61σ- 84σ85σ87σ	53σ59σ61σ- 84σ85σ87σ	62σ64σ76σ- 92σ93σ94 σ
33 (88)	65σ80σ81σ- 89σ90σ93σ	6σ65σ67σ- 89σ92σ93σ	70σ71σ82σ- 98σ99σ101σ
34 (75)	53σ56σ58σ- 76σ79σ80σ	55σ56σ57σ- 76σ79σ80σ	58σ59σ69σ- 83σ86σ88σ
35 (105)	82σ83σ85σ- 106σ107σ110σ	76σ77σ83σ- 106σ107σ109σ	85σ86σ96σ- 117σ118σ119σ
36 (83)	49σ52σ56σ- 84σ85σ86σ	55σ56σ60σ- 84σ86σ87σ	62σ63σ76σ- 92σ93σ94σ
37 (75)	47σ48σ55σ- 76σ77σ78σ	49σ52σ55σ- 76σ77σ78σ	58σ59σ68σ- 84σ86σ87σ
38 (83)	56σ57σ62σ- 84σ85σ87σ	57σ58σ61σ- 84σ85σ87σ	65σ67σ76σ- 92σ93σ94σ
39 (83)	51σ54σ55σ- 85σ86σ89σ	48σ51σ55σ- 85σ86σ89σ	63σ65σ75σ- 93σ95σ96σ
40 (92)	60σ64σ66σ- 94σ95σ98σ	57σ60σ64σ- 94σ95σ98σ	72σ74σ83σ- 102σ103σ104σ
41 (92)	66σ67σ69σ- 93σ94σ95σ	66σ67σ68σ- 93σ94σ95σ	74σ76σ83σ- 102σ106σ107σ
42 (87)	56σ63σ66σ- 88σ89σ91σ	54σ60σ65σ- 88σ89σ91σ	68σ69σ79σ- 97σ98σ99σ
43 (83)	54σ59σ64σ- 84σ85σ86σ	54σ58σ63σ- 84σ85σ86σ	66σ67σ76σ- 93σ94σ96σ

Discussion of the results for the 5-HT$_{2A}$ receptor.

Table 2 shows that the relative importance of variables in Eq. 2 is $Q_{13}^{*,max}$> S_9^E(HOMO-1)*~ S_{20}^N(LUMO+1)*>> η_{14}> F_{16}(HOMO)*>> Q_{20}> S_{21}^E(HOMO)*.

A high 5-HT$_{2A}$ receptor affinity is associated with large negative values for S_9^E(HOMO-1)*, small positive values for S_{20}^N(LUMO+1)*, small (positive) values for $Q_{13}^{*,max}$, large (positive) values for η_{14}, small (positive) values for F_{16}(HOMO)*, large (negative) values for Q_{20} and small negative values for S_{21}^E(HOMO)*.

Atom 9 is a sp^2 nitrogen atom in ring B (Fig. 8). Table 11 shows that (HOMO)$_9$* and (HOMO-1)$_9$* have a π character. A high 5-HT$_{2A}$ receptor affinity is associated with large negative values for S_9^E(HOMO-1)*. Note that this reactivity index is 'facing' the Fukui indices of the empty local MOs of an atom or group of atoms in the receptor[32]. By 'facing' we mean that both terms appear together in Eq. 1. These values are obtained by shifting the energy of (HOMO-1)$_9$* toward zero, making this atom a good electron donor. Nevertheless in this case (HOMO)$_9$* and (HOMO-1)$_9$* coincide with the molecule's (HOMO) and (HOMO-1), making it difficult this approach. Another possibility is to fully localize the molecular (HOMO) and (HOMO-1) on atom 9. Thus, atom 9 seems to interact with

an electron-deficient center (π-cation or π-π interactions). Another possibility is that π electrons of atom 9 participate in a N_9-H_{22}-O hydrogen bond [37].

Atom 20 is a hydrogen atom bonded to N_{12} in the chain linking rings B and C (Fig. 8). All local MOs have a σ nature (Table 13). Table 13 shows that local $(HOMO)_{20}^*$ corresponds to inner occupied molecular orbitals that are energetically very far from the molecular HOMO. Local $(LUMO)_{20}^*$ coincides with the molecular LUMO. Small positive values for $S_{20}^N(LUMO+1)^*$ are associated with high pK values. Note that this reactivity index is 'facing' the Fukui indices of the occupied local MOs of an atom or group of atoms in the receptor[32]. This is indirectly reflected in the fact that the net charge of this atom is positive in all molecules. Here the situation seems to be optimal when atom 20 is a bad electron donor and a bad electron acceptor. An ideal situation would be for $(LUMO+1)_{20}^*$ to match an empty MO of the molecule that has a high energy. Within a static model, it is possible to think that $(HOMO)_{20}^*$ serves as a 'bridge' for the movement of electrons in a possible N_{12}-H_{20}-X hydrogen bond.

Atom 13 is a sp^3 carbon atom bonded to N_{12} and sp^2 C_{14} (Fig. 8). All local MOs have a σ nature (Table 11). $(HOMO)_{13}^*$ coincide with MOs that are energetically close to the molecule's HOMO. $(LUMO)_{13}^*$ coincides with the molecular LUMO. A high pK value is associated with small (positive) values for $Q_{13}^{*,max}$. So, an atom that is a bad charge acceptor would be an optimal situation. That could be achieved with two tactics. One is to make $(HOMO)_{13}^*$ match the molecular HOMO and make the value of $F_{13}(HOMO)^*$ as close as possible to 2.0 (i.e., that the molecular MO is located almost completely on atom 13). The second is to make $(LUMO)_{13}^*$ match an empty MO of the molecule whose energy is as far away from energy zero as possible. We also know that the maximal amount of electronic charge that an electrophile may accept is defined as $(-\mu_{13}^*/\eta_{13}^*)$ where μ_{13}^* is the local electron chemical potential of atom 13 and η_{13}^* is the local atomic hardness of the same atom. Since η_{13}^* is the gap between the energies of (HOMO)13* and $(LUMO)_{13}^*$, the higher the local hardness, the lower $Q_{13}^{*,max}$. This is consistent with the second tactic just mentioned. The first tactic further suggests that atom 13 could be interacting with an electron-deficient site (alkyl or CH-π interactions [37]).

Atom 14 is a sp2 carbon atom in ring C (Fig. 8). Table 12 shows that the local frontier molecular orbitals of atom 14 coincide with or are energetically close to the molecule's frontier orbitals, all having a π nature. A high pK value is associated with large (positive) values for η_{14}. η_{14}^* is the gap between the energies of (HOMO)14* and $(LUMO)_{14}^*$. There are three approaches to obtain larger values for η_{14} (that is always a positive number in this kind of molecules). The first is to replace the current local $(LUMO)_{14}^*$ with an empty MO of the molecule that possesses a much higher energy. This will cause this atom to behave like a bad electron acceptor. The second method is to replace the current $(HOMO)_{14}^*$ with an occupied MO of the molecule that has a much higher energy. This modification will cause atom 14 to behave like a bad electron donor. The third option is a combination of the previous two, making atom 14 a bad donor and a bad electron acceptor. These effects can be studied by various substitutions in the C_{15}-C_{19} atoms of the C ring. An additional possibility is to substitute in the C_{13} atom. The actual theory does not allow us to select one of these three options, but we can assume that this atom is a bad giver and a bad electron acceptor (this atom can undergo π-cation, π-anion, π-π, π-σ and/or π-alkyl interactions[37]).

Atom 16 is a sp^2 carbon atom in ring C (Fig. 8). Table 12 shows that all frontier local molecular orbitals of this atom have a π nature and that either coincide with the frontier OM of the molecule or are energetically very close to them. A high pK value is associated with small (positive) values for $F_{16}(HOMO)^*$. Note that this reactivity index is 'facing' the nucleophilic superdelocalizability of the empty local MOs of an atom or group of atoms in the receptor[32]. Small values for this reactivity index can be obtained by decreasing the localization of this OM on atom 16, making this atom a bad electron donor. This fact can be explained at this level of the model by suggesting that the local occupied MOs are 'clashing' with occupied MOs in the receptor site [38-41]. This suggestion deserves more future analysis.

Atom 21 is a hydrogen atom bonded to N_{12} in the chain linking rings B and C (Fig. 8). All MOs have a σ nature. Table 13 shows that the local $(HOMO)_{21}^*$ corresponds to an occupied MO that is energetically very far from the molecule's HOMO. Local $(LUMO)_{21}^*$ either coincides with the molecule's LUMO or is energetically very close to it. Small negative values for $S_{21}^E(HOMO)^*$ are associated with high pK values. Note that this reactivity index is 'facing' the Fukui indices of the empty local MOs of an atom or group of atoms in the receptor[32]. This means that this atom should behave as a bad electron donor. We can hypothesize that the local $(LUMO)_{21}^*$ of this atom 'allows'

electrons to circulate in an eventual hydrogen bond of the X-H_{21}-N_{12} type and that this circulation is facilitated by the net positive charge of H_{20}. All the suggestions are displayed in the partial 2D pharmacophore of Fig. 33.

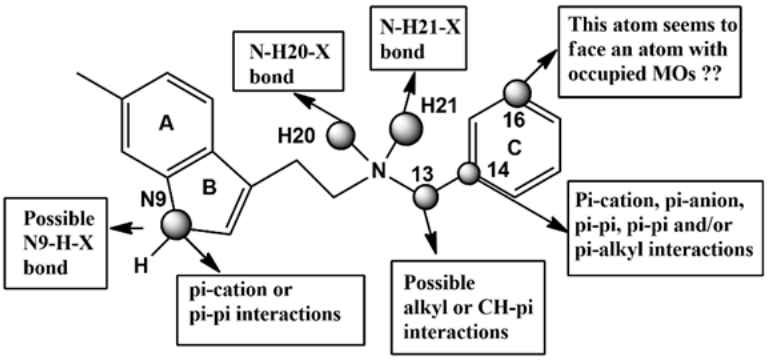

Figure 33: Partial 2D pharmacophore for 5-HT_{2A} receptor affinity

Discussion of the results for the 5-HT_{2B} receptor

Table 4 shows that the importance of variables in Eq. 3 is s_{13}> S_{21}^{E}(HOMO-1)*~ F_{14}(LUMO)*> S_{20}^{N}(LUMO+2)*> S_4^{N}(LUMO)*~ S_{23}^{N}> S_{22}^{N}(LUMO)*> S_6^{N}(LUMO+1)*> S_{21}^{N}> S_{22}^{N}>> S_{13}^{E}(HOMO-2)*.

A high pK value is associated with large (positive) values for F_{14}(LUMO)*, large (positive) values for S_{20}^{N}(LUMO+2)*, large (negative) values for S_{21}^{E}(HOMO-1)*, small (positive) values for S_4^{N}(LUMO)*, large positive values for S_{23}^{N}, small (positive) values for s_{13}, small (positive) values for S_6^{N}(LUMO+1)*, large positive values for S_{22}^{N}(LUMO)*, large positive values for S_{22}^{N}, small (positive) values for S_{21}^{N} and small (negative) values for S_{13}^{E}(HOMO-2)*.

Atom 14 is a sp^2 carbon atom in ring C (Fig. 8). Table 12 shows that the local frontier molecular orbitals of atom 14 coincide with or are energetically close to the molecule's frontier molecular orbitals, having all a π nature. A high pK value is associated with large positive values for F_{14}(LUMO)*. Note that this reactivity index is 'facing' the electrophilic superdelocalizability of the occupied local MOs of an atom or group of atoms in the receptor[32]. These values are obtained by augmenting the percentage of localization of $(LUMO)_{14}$* on this atom. Therefor we may suggest that this atom is facing an electron-rich center. We suggest that atom 14 is participating in π-anion, π-π and/or π-alkyl interactions[37].

Atom 20 is a hydrogen atom bonded to N_{12} in the chain linking rings B and C (Fig. 8). All local MOs have a σ nature (Table 13). Local $(HOMO)_{20}^{*}$ corresponds to molecules' inner occupied MOs that are energetically very far from the HOMO. Local $(LUMO)_{20}^{*}$ coincides with empty molecular MOs that are energetically close to the LUMO. A high pK value is associated with large (positive) values for S_{20}^{N}(LUMO+2)*. Note that this reactivity index is 'facing' the Fukui index of the occupied local MOs of an atom or group of atoms in the receptor[32]. These values are obtained by lowering the $(LUMO+2)_{20}^{*}$ energy or by rising the localization of this empty MO on atom 20, making it more reactive. Note that this will shift the energies of $(LUMO)_{20}^{*}$ and $(LUMO+1)_{20}^{*}$ toward zero. Again we are in the situation where H_{20} seems to play a role in the formation of a X-H_{20}-N_{12} hydrogen bond[37].

Atom 21 is a hydrogen atom bonded to N_{12} in the chain linking rings B and C (Fig. 8). All MOs have a σ nature (Table 13). Local $(HOMO)_{21}^{*}$ corresponds to molecules' inner occupied MOs that are energetically very far from the HOMO. Local $(LUMO)_{21}^{*}$ coincides with empty molecular MOs that are energetically close to the LUMO. A high pK value is associated with large (negative) values for S_{21}^{E}(HOMO-1)*. Note that this reactivity index is 'facing' the Fukui index of the empty local MOs of an atom or group of atoms in the receptor[32]. These values are obtained shifting the $(HOMO-1)_{21}^{*}$ toward zero. Note that this will also shift the energy of $(HOMO)_{21}^{*}$ toward zero. The only suggestion we may present for the moment is that atom 21 is participating in a N_{12}-H_{21}-X hydrogen bond where X should be an electron-acceptor[37].

Atom 4 is a sp^2 carbon atom shared by rings A and B (Fig. 8). Table 10 shows that local $(HOMO)_4^{*}$ coincides with the molecular HOMO, and that local $(LUMO)_4^{*}$ corresponds to a higher empty molecular MO and not to the

molecular LUMO. A high pK value is associated with small (positive) values for S_4^N(LUMO)*. Note that this reactivity index is 'facing' the Fukui index of the occupied local MOs of an atom or group of atoms in the receptor[32]. Small (positive) numerical values for S_4^N(LUMO)* are obtained by increasing $(LUMO)_4^*$ energy, making this atom a bed electron acceptor. These values are obtained by increasing the $(LUMO)_4^*$ energy. This suggests that there could be a repulsive interaction between occupied MOs of both partners [40, 41].

Atom 23 is the first atom of the substituent attached to C_1 (H or O from OMe in this case, see Table 1 and Figs. 1 and 8). In the case of H, all local MOs have a σ nature. A high pK value is associated with large positive values for S_{23}^N. Note that this reactivity index is 'facing' the Fukui index of the occupied local MOs of an atom or group of atoms in the receptor[32]. These values are obtained by shifting the energies of the first empty local MOs toward zero, making them more reactive. Therefore, atom 23 should be interacting with an electron-rich center at least in the case of an H atom. We suggest that in this case a carbon H-bond could occur (this suggestion is made despite the fact that in the definition of a carbon hydrogen bond it is stated that "a carbon atom is considered a donor either if it is in an acetylene group or if it is adjacent to an oxygen or nitrogen atom")[37]. Another possibility is that the empty σ MOs of atom 23 interact weakly with the occupied MOs of the site. It should be made clear that when a reactivity index of two atoms as different as hydrogen and oxygen appears inside a QSAR equation, there are always problems of interpretation. We have left an equation of this kind to show that perhaps some theoretical development is missing to explain this fact, or else the two atoms are interacting with two different sites. For that reason, a third suggestion is that the lone pairs of the oxygen atom may be interacting through a hydrogen bond [37].

Atom 13 is a sp^3 carbon atom bonded to N_{12} and sp^2 C_{14} (Fig. 8). All local MOs have a σ nature (Table 11). Local $(HOMO)_{13}^*$ corresponds to molecules' inner occupied MOs that are not energetically very far from the HOMO. Local $(LUMO)_{13}^*$ coincides with the molecular LUMO. A high pK value is associated with small (negative) values for S_{13}^E(HOMO-2)*. Note that this reactivity index is 'facing' the Fukui index of the empty local MOs of an atom or group of atoms in the receptor[32]. These values are obtained by modifying the localization of the molecule's MOs in such a way that local $(HOMO-2)_{13}^*$ coincides with an inner occupied molecular MO. If we accept that the condition imposed on $(HOMO-2)_{13}^*$ must be applied to $(HOMO-1)_{13}^*$ and $(HOMO)_{13}^*$, then atom 13 should be a bad electron donor. This is not new because, given the location of atom 13 within the molecule, charge transfer is not expected. For this sp^3 carbon atom we suggest alkyl, σ-π, weak carbon H-bond and/or alkyl-π interactions[37].

Atom 6 is a sp^2 carbon atom in ring A (Fig. 8). All local frontier MOs have a π nature. $(HOMO)_6^*$ coincides with the molecular HOMO, and $(LUMO)_6^*$ coincides with an empty MO different from the molecular LUMO. A high pK value is associated with small (positive) values for S_6^N(LUMO+1)*. Note that this reactivity index is 'facing' the Fukui index of the occupied local MOs of an atom or group of atoms in the receptor[32]. We expect that this atom will interact with an electron-rich center. But the small (positive) values for S_6^N(LUMO+1)* are obtained by modifying the localization of the molecule's empty MOs in such a way that local $(LUMO+1)_6^*$ coincides with an upper empty MO of the molecule, making this atom less prone to interact with electron-rich centers. We suggest that the occupied local MOs of atom 16 have repulsive interactions with the occupied MOs of the site [40, 41].

Atom 22 is a hydrogen atom bonded to N_9 (Fig. 8). All MOs have a σ nature (Table 13). Local $(HOMO)_{22}^*$ corresponds to molecules' inner occupied MOs that are energetically far from the HOMO. Local $(LUMO)_{22}^*$ coincides with empty molecular MOs that are energetically far from the LUMO. A high pK value is associated with large positive values for S_{22}^N(LUMO)*. Note that this reactivity index is 'facing' the Fukui index of the occupied local MOs of an atom or group of atoms in the receptor[32]. An ideal situation would be when $(LUMO)_{22}^*$ coincides with the molecule's LUMO and the corresponding Fukui index has a high numerical value. Within a static model, it is possible to think that $(LUMO)_{22}^*$ serves as a 'bridge' for the movement of electrons in a possible N_9-H_{22}-X hydrogen bond[37].

All the suggestions are displayed in the partial 2D pharmacophore of Fig. 34.

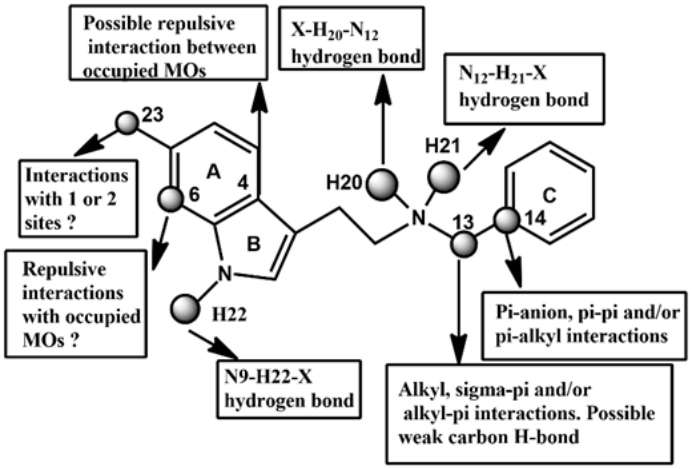

Figure 34: Partial 2D pharmacophore for 5-HT$_{2B}$ receptor affinity

Discussion of the results for the 15 lowest experimental values of 5-HT$_{2C}$ receptor affinity

Table 6 shows that the importance of variables in Eq. 4 is s_{16}> S_{10}^{N}(LUMO+1)*>> F_{17}(HOMO-2)*> F_{10}(LUMO)*>> Q_{17}.

A high pK value is associated with small (positive) numerical values for s_{16}, large (positive) numerical values for S_{10}^{N}(LUMO+1)*, small (positive) numerical values for F_{10}(LUMO)*, small (negative) numerical values for F_{17}(HOMO-2)* and a positive net charge for atom 17.

Atom 16 is a sp^2 carbon atom in ring C (Fig. 8). Table 12 shows that all frontier local molecular orbitals of this atom have a π nature and that either coincide with the frontier OM of the molecule or are energetically very close to them. A high pK value is associated with small (positive) values for F_{16}(HOMO)*, and with small (positive) numerical values for s_{16}. Note that this reactivity index is 'facing' the nucleophilic superdelocalizability of the empty local MOs of an atom or group of atoms in the receptor[32]. We can explain this fact by suggesting that, despite the fact that this atom is facing empty MOs of the receptor's atom, it seems that there is a negative interaction between the occupied MOs of both atoms [40, 41]. It is difficult to suggest possible interactions. On the other hand, considering that $s_{16}=1/\eta_{16}$, a large gap between $(HOMO)_{16}^{*}$ and $(LUMO)_{16}^{*}$ can be obtained by changing (by substitution) the localization of $(HOMO)_{16}^{*}$ in such a way that it coincides with a with an occupied MO of the molecule having a much larger ionization potential.

Atom 10 is a sp^3 carbon atom bonded to C_7 and sp^2 C_{11} (Fig. 8). All local MOs have a σ nature (Table 11). Local $(HOMO)_{10}^{*}$ corresponds to molecules' HOMO. Local $(LUMO)_{10}^{*}$ coincides with empty molecular MOs that are energetically far from the LUMO. A high pK value is associated with large (positive) numerical values for S_{10}^{N}(LUMO+1)* and with small (positive) numerical values for F_{10}(LUMO)*. Note that this reactivity index is 'facing' the Fukui index of the occupied local MOs of an atom or group of atoms in the receptor[32]. These values are obtained by shifting the $(LUMO+1)_{10}^{*}$ energy toward zero, making empty MOs more reactive. Possible interactions are alkyl and π-alkyl ones[37]. Decreasing the numerical value of F_{10}(LUMO)* is equivalent to diminish the localization of the corresponding MO.

Atom 17 is a sp^2 carbon atom in ring C (Fig. 8). Table 12 shows that the frontier local MOs of this atom have a π nature. Local $(HOMO)_{17}^{*}$ corresponds to molecules' inner occupied MOs that are not energetically far from the HOMO. Local $(LUMO)_{17}^{*}$ coincides with the LUMO. A high pK value is associated with small (negative) numerical values for F_{17}(HOMO-2)*, and with a positive net charge for this atom. Both conditions are complementary. Note that this reactivity index is 'facing' the nucleophilic superdelocalizability of the empty local MOs of an atom or group of atoms in the receptor[32]. These values are obtained by diminishing the localization of $(HOMO-2)_{17}^{*}$ on this atom. Because the interaction of an atom with a positive net charge with a site that appears to be an electron acceptor (either by charge transfer or by weak interaction between MOs) should be repulsive, we can only suggest

for the moment the existence of some possible repulsive interaction. In this case, more theoretical research is needed.

All the suggestions are displayed in the partial 2D pharmacophore of Fig. 35.

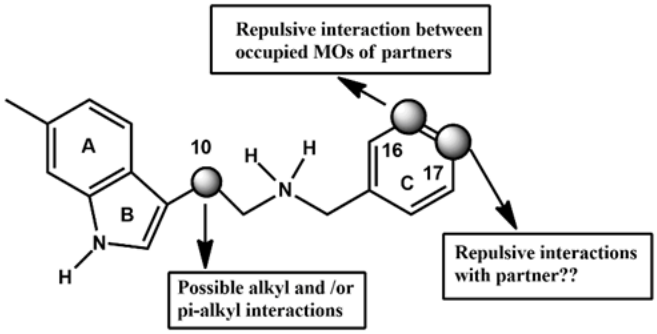

Figure 35: Partial 2D pharmacophore for the 15 lowest experimental values of 5-HT$_{2C}$ receptor affinity

Discussion of the results for the 26 highest experimental values of 5-HT$_{2C}$ receptor affinity

Table 8 shows that the importance of variables in Eq. 5 is F_8(LUMO+1)*>> S_{18}^E(HOMO-1)*> S_{13}^E(HOMO-1)*> S_6^N> S_4^N(LUMO+2)*> F_6(HOMO-2)*~ F_5(LUMO)*.

A high pK value is associated with large (positive) numerical values for F_8(LUMO+1)*, small (positive) numerical values for F_6(HOMO-2)*, small (negative) numerical values for S_{18}^E(HOMO-1)*, small (negative) numerical values for S_{13}^E(HOMO-1)*, small (positive) numerical values for S_4^N(LUMO+2)*, large (positive) numerical values for S_6^N and large (positive) numerical values for F_5(LUMO)*.

Atom 8 is a sp^2 carbon atom in ring B (Fig. 8). Table 11 shows that all frontier local MOs have a π nature. $(HOMO)_8^*$ coincides with the molecular HOMO. Local $(LUMO)_8^*$ corresponds to a higher empty molecular MO not energetically far from the molecular LUMO. A high pK value is associated with large (positive) numerical values for F_8(LUMO+1)*. Note that this reactivity index is 'facing' the electrophilic superdelocalizability of the occupied local MOs of an atom or group of atoms in the receptor[32]. These values are obtained by increasing the localization of $(LUMO+1)_8^*$ in such a way that in the best case F_8(LUMO+1)* = 2. Possible interactions are π-π and/or π-anion[37].

Atom 6 is a sp^2 carbon atom in ring A (Fig. 8). All local frontier MOs have a π nature (Table 10). $(HOMO)_6^*$ coincides with the molecular HOMO, and $(LUMO)_6^*$ coincides with an empty MO different from the molecular LUMO. A high pK value is associated with small (positive) numerical values for F_6(HOMO-2)*. Note that this reactivity index is 'facing' the nucleophilic superdelocalizability of the empty local MOs of an atom or group of atoms in the receptor[32]. The values are obtained by diminishing the localization of $(HOMO-2)_6^*$ in such a way that F_6(HOMO-2)* -› 0.0. If F_6(HOMO-2)*=0 this means that this MO will be replaced by an inner occupied MO of the molecule having a much larger ionization potential. All these facts can be explained by suggesting that atom 6 is interacting with an electron-deficient site but with a limit given by possible repulsive interactions of occupied MOs of both partners [38, 39]. Possible interactions are π-π and/or π-cation[37].

Atom 18 is a sp^2 carbon atom in ring C (Fig. 8). Table 12 shows that the local $(HOMO)_{18}^*$ corresponds to a molecular inner occupied MO that is not energetically far from the HOMO. Local $(LUMO)_{18}^*$ coincides with the molecular LUMO. All frontier MOs have a π nature. A high pK value is associated with small (negative) numerical values for S_{18}^E(HOMO-1)*. Note that this reactivity index is 'facing' the Fukui index of the empty local MOs of an atom or group of atoms in the receptor[32]. This suggests that only $(HOMO)_{18}^*$ is interacting with the site through π-π and/or π-cation interactions[37]

Atom 13 is a sp^3 carbon atom bonded to N_{12} and sp^2 C_{14} (Fig. 8). All local MOs have a σ nature (Table 11). Local $(HOMO)_{13}^*$ corresponds to molecules' inner occupied MOs that are not energetically very far from the HOMO. Local $(LUMO)_{13}^*$ coincides with the molecular LUMO. A high pK value is associated with small (negative) numerical values for S_{13}^E(HOMO-1)*. Note that this reactivity index is 'facing' the Fukui index of the empty local MOs of an atom or group of atoms in the receptor[32]. This atom could interact with the site through a weak carbon H-bond, alkyl, σ-π and/or alkyl-π interactions.

Atom 4 is a sp^2 carbon atom shared by rings A and B (Fig. 8). Table 10 shows that local $(HOMO)_4$* coincides with the molecular HOMO, and that local $(LUMO)_4$* corresponds to a higher empty molecular MO and no to the molecular LUMO. All MOs have a π nature (Table 10). A high pK value is associated with small (positive) numerical values for S_4^N(LUMO+2)*. Note that this reactivity index is 'facing' the Fukui index of the occupied local MOs of an atom or group of atoms in the receptor[32]. This suggests that atom 4 is interacting with the site only through $(LUMO)_4$* and $(LUMO+1)_4$* through π-π and/or π-anion interactions[37].

Atom 5 is a sp^2 carbon atom belonging to rings A and B (Fig. 8). Table 10 shows that local $(HOMO)_5$* coincides with the molecular HOMO. Local $(LUMO)_5^*$ corresponds to a higher empty molecular MO not energetically far from the molecular LUMO. All local frontier MOs have a π nature. A high pK value is associated with large (positive) numerical values for F_5(LUMO)*. Note that this reactivity index is 'facing' the nucleophilic superdelocalizability of the empty local MOs of an atom or group of atoms in the receptor[32]. For the moment we have not an acceptable explanation.

All the suggestions are displayed in the partial 2D pharmacophore of Fig. 36.

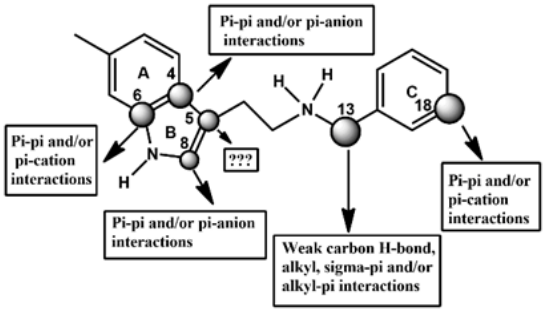

Figure 36: Partial 2D pharmacophore for the 26 highest experimental values of 5-HT_{2C} receptor affinity

In summary, we have obtained statistically significant results for the all the receptor data analyzed. We have not a clear explanation for the separation of the 5-HT_{2C} data into two separate sets. Different modes of binding or different receptor site conformations are some possibilities. The data employed in this paper will be useful for evaluating the new developments in the model

No part of this paper has been written with IA tools.

References

[1]. Lin, J.; Liu, W.; Guan, J.; Cui, J.; Shi, R.; Wang, L.; Chen, D.; Liu, Y. Latest updates on the serotonergic system in depression and anxiety. Front. Synaptic Neurosci. 2023, 15.

[2]. Gómez-Jeria, J. S.; Robles-Navarro, A.; Jaramillo-Hormazábal, I. A DFT analysis of the relationships between electronic structure and activity at D2, 5-HT1A and 5-HT2A receptors in a series of Triazolopyridinone derivatives. Chemistry Research Journal 2022, 7, 6-28.

[3]. Gómez-Jeria, J. S.; Olarte-Lezcano, L. On the relationships between electronic structure and 5-HT2A, 5-HT2C and D2 receptor affinities in a group of 2-aryl tryptamines. A DFT study. Chemistry Research Journal 2022, 7, 14-35.

[4]. Gómez-Jeria, J. S.; Robles-Navarro, A.; Soza-Cornejo, C. A note on the relationships between electronic structure and serotonin 5-HT1A receptor binding affinity in a series of 4-butyl-arylpiperazine-3-(1H-indol-3-yl)pyrrolidine-2,5-dione derivatives. Chemistry Research Journal 2021, 6, 76-88.

[5]. Gómez-Jeria, J. S.; Rojas-Candia, V. A DFT Investigation of the Relationships between Electronic Structure and D2, 5-HT1A, 5-HT2A, 5-HT6 and 5-HT7 Receptor Affinities in a group of Fananserin derivatives. Chemistry Research Journal 2020, 5, 37-58.

[6]. Gómez-Jeria, J. S.; Gatica-Díaz, N. A preliminary quantum chemical analysis of the relationships between electronic structure and 5-HT1A and 5-HT2A receptor affinity in a series of 8-acetyl-7-hydroxy-4-methylcoumarin derivatives. Chemistry Research Journal 2019, 4, 85-100.

[7]. Gómez-Jeria, J. S.; Moreno-Rojas, C.; Castro-Latorre, P. A note on the binding of N-2-methoxybenzyl-phenethylamines (NBOMe drugs) to the 5-HT2C receptors. Chemistry Research Journal 2018, 3, 169-175.

[8]. Gómez-Jeria, J. S.; Abuter-Márquez, J. A Theoretical Study of the Relationships between Electronic Structure and 5-HT1A and 5- HT2A Receptor Binding Affinity of a group of ligands containing an isonicotinic nucleus. Chemistry Research Journal 2017, 2, 198-213.

[9]. Gómez-Jeria, J. S.; Robles-Navarro, A. A Quantum Chemical Study of the Relationships between Electronic Structure and cloned rat 5-HT2C Receptor Binding Affinity in N-Benzylphenethylamines. Research Journal of Pharmaceutical, Biological and Chemical Sciences 2015, 6, 1358-1373.

[10]. Gómez-Jeria, J. S.; Robles-Navarro, A. DFT and Docking Studies of the Relationships between Electronic Structure and 5-HT2A Receptor Binding Affinity in N-Benzylphenethylamines. Research Journal of Pharmaceutical, Biological and Chemical Sciences 2015, 6, 1811-1841.

[11]. Gómez-Jeria, J. S.; Robles-Navarro, A. A Note on the Docking of some Hallucinogens to the 5-HT2A Receptor. Journal of Computational Methods in Molecular Design 2015, 5, 45-57.

[12]. Richter, P.; Morales, A.; Gomez-Jeria, J. S.; Morales-Lagos, D. Electrochemical study of the hallucinogen (±)-1-(2,5-dimethoxy-4-nitrophenyl)-2-aminopropane. Analyst 1988, 113, 859-863.

[13]. Gómez-Jeria, J. S.; Cassels, B. K.; Saavedra-Aguilar, J. C. A quantum-chemical and experimental study of the hallucinogen (±)-1-(2,5-dimethoxy-4-nitrophenyl)-2-aminopropane (DON). European Journal of Medicinal Chemistry 1987, 22, 433-437.

[14]. Gómez-Jeria, J. S.; Morales-Lagos, D.; Cassels, B. K.; Saavedra-Aguilar, J. C. Electronic structure and serotonin receptor binding affinity of 7-substituted tryptamines. Quantitative Structure-Activity Relationships 1986, 5, 153-157.

[15]. Gómez-Jeria, J. S.; Cassels, B. K.; Clavijo, R. E.; Vargas, V.; Quintana, R.; Saavedra-Aguilar, J. C. Spectroscopic characterization of a new hallucinogen: 1-(2,5-dimethoxy-4-nitrophenyl)-2-aminipropane (DON). Microgram (DEA) 1986, 19, 153-162.

[16]. Gómez-Jeria, J. S.; Morales-Lagos, D.; Rodriguez-Gatica, J. I.; Saavedra-Aguilar, J. C. Quantum-chemical study of the relation between electronic structure and pA2 in a series of 5-substituted tryptamines. International Journal of Quantum Chemistry 1985, 28, 421-428.

[17]. Gómez-Jeria, J. S.; Morales-Lagos, D. R. Quantum chemical approach to the relationship between molecular structure and serotonin receptor binding affinity. Journal of Pharmaceutical Sciences 1984, 73, 1725-1728.

[18]. Gómez-Jeria, J. S.; Morales-Lagos, D. The mode of binding of phenylalkylamines to the Serotonergic Receptor. In QSAR in design of Bioactive Drugs, Kuchar, M., Ed. Prous, J.R.: Barcelona, Spain, 1984; pp 145-173.

[19]. Gómez-Jeria, J. S. Approximate Molecular Electrostatric Potentials of Protonated Mescaline Analogues. Acta sud Americana de Química 1984, 4, 1-9.

[20]. Halberstadt, A. L. Pharmacology and Toxicology of N-Benzylphenethylamine ("NBOMe") Hallucinogens. Current topics in behavioral neurosciences 2017, 32, 283-311.

[21]. Halberstadt, A. L. Pharmacology and Toxicology of N-Benzylphenethylamine (“NBOMe”) Hallucinogens. In Neuropharmacology of New Psychoactive Substances (NPS): The Science Behind the Headlines, Baumann, M. H.; Glennon, R. A.; Wiley, J. L., Eds. Springer International Publishing: Cham, 2017; pp 283-311.

[22]. Toro-Sazo, M.; Brea, J.; Loza, M. I.; Cimadevila, M.; Cassels, B. K. 5-HT2 receptor binding, functional activity and selectivity in N-benzyltryptamines. PLOS ONE 2019, 14, e0209804.

[23]. Gómez Jeria, J. S. La Pharmacologie Quantique. Bollettino Chimico Farmaceutico 1982, 121, 619-625.

[24]. Gómez-Jeria, J. S. On some problems in quantum pharmacology I. The partition functions. International Journal of Quantum Chemistry 1983, 23, 1969-1972.

[25]. Gómez-Jeria, J. S. The use of competitive ligand binding results in QSAR studies. Il Farmaco; edizione scientifica 1985, 40, 299-302.

[26]. Gómez-Jeria, J. S. Modeling the Drug-Receptor Interaction in Quantum Pharmacology. In Molecules in Physics, Chemistry, and Biology, Maruani, J., Ed. Springer Netherlands: 1989; Vol. 4, pp 215-231.
[27]. Gómez-Jeria, J. S.; Ojeda-Vergara, M. Parametrization of the orientational effects in the drug-receptor interaction. Journal of the Chilean Chemical Society 2003, 48, 119-124.
[28]. Gómez-Jeria, J. S. Elements of Molecular Electronic Pharmacology (in Spanish). 1st ed.; Ediciones Sokar: Santiago de Chile, 2013; p 104.
[29]. Gómez-Jeria, J. S. A New Set of Local Reactivity Indices within the Hartree-Fock-Roothaan and Density Functional Theory Frameworks. Canadian Chemical Transactions 2013, 1, 25-55.
[30]. Gómez-Jeria, J. S.; Castro-Latorre, P.; Moreno-Rojas, C. Dissecting the drug-receptor interaction with the Klopman-Peradejordi-Gómez (KPG) method. II. The interaction of 2,5-dimethoxyphenethylamines and their N-2-methoxybenzyl-substituted analogs with 5-HT2A serotonine receptors. Chemistry Research Journal 2018, 4, 45-62.
[31]. Gómez-Jeria, J. S.; Crisóstomo-Cáceres, S. R.; Robles-Navarro, A. On the compatibility between formal QSAR results and docking results: the relationship between electronic structure and H5N1 (A/goose/Guangdong/SH7/2013) neuraminidase inhibition by some Tamiflu derivatives as an example. Chemistry Research Journal 2021, 6, 46-59.
[32]. Gómez-Jeria, J. S. A Note on Local Molecular Orbitals and Non-linear terms in the Klopman-Peradejordi-Gómez QSAR method. Chemistry Research Journal 2024, 9, 50-57.
[33]. Frisch, M. J.; Trucks, G. W.; Schlegel, H. B.; Scuseria, G. E.; Robb, M. A.; Cheeseman, J. R.; Scalmani, G.; Barone, V.; Petersson, G. A.; Nakatsuji, H.; Li, X.; Caricato, M.; Marenich, A. V.; Bloino, J.; Janesko, B. G.; Gomperts, R.; Mennucci, B.; Hratchian, H. P. Gaussian 16 16Rev. A.03, Gaussian: Pittsburgh, PA, USA, 2016.
[34]. Gómez-Jeria, J. S. D-Cent-QSAR: A program to generate Local Atomic Reactivity Indices from Gaussian16 log files, v. 1.0; Santiago, Chile, 2020.
[35]. Gómez-Jeria, J. S. An empirical way to correct some drawbacks of Mulliken Population Analysis (Erratum in: J. Chil. Chem. Soc., 55, 4, IX, 2010). Journal of the Chilean Chemical Society 2009, 54, 482-485.
[36]. Statsoft. Statistica v.10, 2300 East 14 th St. Tulsa, OK 74104, USA, 2011.
[37]. Gómez-Jeria, J. S.; Robles-Navarro, A.; Kpotin, G.; Garrido-Sáez, N.; Gatica-Díaz, N. Some remarks about the relationships between the common skeleton concept within the Klopman-Peradejordi-Gómez QSAR method and the weak molecule-site interactions. Chemistry Research Journal 2020, 5, 32-52.
[38]. Hoffmann, R. How Chemistry and Physics Meet in the Solid State. 1987, 26, 846-878.
[39]. Hoffmann, R. A chemical and theoretical way to look at bonding on surfaces. Reviews of Modern Physics 1988, 60, 601-628.
[40]. Joselevich, E. Electronic Structure and Chemical Reactivity of Carbon Nanotubes: A Chemist's View. ChemPhysChem 2004, 5, 619-624.
[41]. Joselevich, E. Chemistry and Electronics of Carbon Nanotubes Go Together. Angewandte Chemie International Edition 2004, 43, 2992-2994.